Sex-dependent, lateralized engagement of anterior insular cortex inputs to the dorsolateral striatum in binge alcohol drinking

David L. Haggerty[1], PhD, Brady K. Atwood, PhD[1,2]

[1]Department of Pharmacology & Toxicology, Indiana University School of Medicine, Indianapolis,
IN, 46202, USA
[2]Stark Neurosciences Research Institute, Indiana University School of Medicine, Indianapolis,
IN, 46202, USA

Corresponding Author:
Brady K. Atwood, PhD
Indiana University School of Medicine
Neuroscience Research Building - Room 400C
320 West 15th St
Indianapolis, IN 46202
Phone: 317-274-8917
Email: bkatwood@iu.edu

Abstract

How does alcohol consumption alter synaptic transmission across time, and do these alcohol-induced neuroadaptations occur similarly in both male and female mice? Previous work shows that anterior insular cortex (AIC) projections to the dorsolateral striatum (DLS) are uniquely sensitive to alcohol-induced neuroadaptations in male, but not female mice, and play a role in governing binge alcohol consumption in male mice. Here, by using high-resolution behavior data paired with *in-vivo* fiber photometry, we show how similar levels of alcohol intake are achieved via different behavioral strategies across sex, and how inter-drinking session thirst states predict future alcohol intakes in females, but not males. Further, we show how presynaptic calcium activity recorded from AIC synaptic inputs in the DLS across 3 weeks of water consumption followed by 3 weeks of binge alcohol consumption change across, fluid, time, sex, and brain circuit lateralization. By time-locking presynaptic calcium activity from AIC inputs to the DLS to peri-initiation of drinking events we also show that AIC inputs into the left DLS robustly encode binge alcohol intake behaviors relative to water consumption and AIC inputs into the right DLS in males, but not females. These findings suggest a fluid-, sex- and lateralization-dependent role for the engagement of AIC inputs into the DLS that encode binge alcohol consumption behaviors and further contextualize alcohol-induced neuroadaptations at AIC inputs to the DLS.

Introduction

Binge alcohol consumption, defined as consuming 4 to 5 or more drinks in about two hours for females and males, respectively, represents a large proportion of the deaths associated with problematic alcohol use and is one of the strongest risk factors for developing alcohol use disorder (AUD) (Mokdad, Marks et al. 2004, Addolorato, Vassallo et al. 2018, Kanny, Naimi et al. 2018). Binge drinking is particularly prevalent amongst young adults, especially among females who have been increasing their alcohol use rates year on year for the past half-decade (Keyes, Jager et al. 2019, White 2020).

Modeling binge drinking in rodent animal models is largely accomplished through the behavioral paradigm, Drinking in the Dark (DID), in which mice have *ad libitum* access to alcohol (20% v/v) in their home cage for two-hour sessions, 3 hours into their dark-light cycle for 3 to 4 days a week, and for one 4-hour “binge” session for a single day, followed by 2 or 3 days of abstinence from alcohol (Thiele and Navarro 2014). This procedure has great construct and predictive validity for human binge drinking. Mice display similar drinking patterns to humans like front-loading behavior wherein they consume larger amounts of alcohol early in the task compared to later in the task (Ardinger, Lapish et al. 2022). DID also successfully induces pharmacologically relevant levels of blood alcohol content (BAC) in mice that is equivalent to the legal intoxication limit in humans (Barkley-Levenson and Crabbe 2014, Huynh, Arabian et al. 2019).

It is also commonly observed that female mice tend to drink more than males across a wide range of alcohol consumption models, including DID (Blednov, Metten et al. 2005, Hwa, Chu et al. 2011, Satta, Hilderbrand and Lasek 2018, Sneddon, White and Radke 2019). Possible reasons are that females tend to drink more than males is due to an increased sensitivity to the rewarding and decreased sensitivity to the aversive properties of alcohol, different pharmacokinetic and pharmacodynamic properties of alcohol, and differences in sex hormone expression levels, such as estrogen which fluctuates across the menstrual cycle (Czerniak 2001, Overstreet, Knapp and Breese 2004, Schramm-Sapyta, Walker et al. 2009, Finn, Helms et al. 2018, Sneddon, White and Radke 2019, Vandegrift, Hilderbrand et al. 2020, Elvig, McGinn et al. 2021). Yet,

there are also reported instances in which male and female mice consume identical amounts of alcohol in these drinking models, such as for mice genetically selected to consume high binge levels of alcohol (Savarese, Ozburn et al. 2021). And, while it is known that estrogen plays a role in increasing alcohol intakes in some models, there is evidence to suggest there is no effect of estrous cycle on alcohol intake specifically during DID (Satta, Hilderbrand and Lasek 2018).

Nonetheless, when female sex-dependent differences in alcohol intake are present during DID, they are often solely reported in comparison to males and/or other experimental controls (*e.g.*, ovariectomized mice). In some cases, these measures of quantitative intake are also reported in combination with how BACs differ by sex, but ultimately these two metrics are often the only two reported measures of how animals consume alcohol differently by sex. Thus, there remains very little knowledge on the behavioral strategies used to achieve alcohol intakes across sexes.

Additionally, the neural circuitry that underlies binge drinking remains poorly understood, and descriptions of sex differences for neural circuits currently implicated in binge alcohol consumption remain even more elusive. Of the neural circuits implicated in binge drinking, only a few of these studies to date have included sex as a factor in their analyses (Rinker, Marshall et al. 2017, Ferguson, Zhang et al. 2019, Siciliano, Noamany et al. 2019, Burnham, Chaimowitz et al. 2021, Dornellas, Burnham et al. 2021, Levine, Skelly et al. 2021, Haggerty, Munoz et al. 2022).

Previous work from our laboratory that investigates such circuitry shows that alcohol uniquely alters anterior insular cortex (AIC) inputs into the dorsolateral striatum (DLS) via synaptic alterations in mu opioid and ionotropic glutamate receptors in male mice (Munoz, Fritz et al. 2018, Haggerty, Munoz et al. 2022). Female mice displayed no alcohol-induced changes in ionotropic glutamate receptor function. Optogenetically activating these AIC inputs to DLS inputs during DID also reduces how much alcohol male mice binge consume.

To further detail the sex differences displayed between male and female mice in DID and build on our understanding of how AIC inputs into the DLS are altered by binge alcohol exposure across time, fluid, and sex, we measured detailed drinking behaviors

and presynaptic calcium activity at AIC inputs into the DLS for 3 weeks of water drinking followed by 3 weeks of binge alcohol drinking. Here, we show that male and females consume water identically, both in amount and behavioral strategy. Next, we described how the drinking mechanics and patterns differ between females and males that binge similar levels of alcohol, such that female mice consume alcohol more efficiently. Also, by measuring inter-DID session water intakes, we show how female, but not male, thirst states predict future alcohol intake. Finally, using intersectional genetic manipulations, we expressed a genetically encoded calcium indicator (GCaMP), bilaterally and exclusively in AIC inputs to the DLS to measure how presynaptic AIC input activity changes across time, sex, fluid, and brain circuit lateralization. By recording GCaMP activity from AIC inputs bilaterally in the DLS, we show that the AIC inputs into the left DLS strongly encode binge alcohol drinking in males. Further, increasing history of alcohol binge drinking alters calcium dynamics in male left AIC inputs into the DLS, suggesting decreased left AIC input engagement as a function of increased drinking history. Together, we establish detailed sex-differences in the behavioral strategies females use to binge consume similar amounts of alcohol compared to males. And, we describe how AIC inputs to the left DLS encode binge alcohol drinking and how the engagement of these inputs changes over the course of binge drinking history across sex, time, and circuit lateralization. Together these findings represent targets for future pharmacotherapies and therapeutic modalities that seek to leverage the unique alcohol-induced changes to AIC inputs into the DLS to create more targeted, efficacious treatment approaches for those experiencing AUD.

Materials and Methods

Animals

Animal care and experimental protocols for this study were approved by the Institutional Animal Care and Use Committee at the Indiana University School of Medicine and all guidelines for ethical protocols and care of experimental animals established by the National Institutes of Health (Bethesda, MD) were followed. Male and Female C57BL/6J mice were ordered from the Jackson Laboratory (Bar Harbor, ME). Animals arrived at 6 weeks of age and were allowed to acclimate to the animal facility for at least 1 week before any surgery was performed. All animals were single housed in a standard 12 hr

111 light/dark cycle (lights on at 08:00 hr). Humidity in the vivarium was held constant at
112 50% and food and water were available *ad libitum*.

113 ***Stereotaxic surgeries***

114 All surgeries were conducted under aseptic conditions using an ultra-precise small
115 animal stereotaxic instrument (David Kopf Instruments, Tujunga, CA). Animals were
116 anesthetized using isoflurane (3% for induction, 1.0–1.5% for maintenance at a flow rate
117 of 25–35 ml/min of oxygen depending on body weight at the time of surgery). Viral
118 injections were performed using a 33-gauge microinjection needle (Hamilton Company,
119 Reno, NV). Animals were treated post-operatively for 72 hr with daily injections of
120 carprofen (5 mg/kg) and topical lidocaine on the surgical incision. Animals were allowed
121 to recover for at least 1 week before behavioral assays began. Animals were assigned
122 to groups randomly and after surgery animal IDs were re-coded to blind experimenters
123 to viral expression status.

124 All mice were injected bilaterally with AAV9-syn-FLEX-jGCaMP7s-WPRE (Addgene,
125 104491-AAV9) in the AIC at coordinates A/P: +2.25, M/L: ±2.25, D/V: −3.10 (100
126 nl/injection, 25 nl/min infusion rate) and AAVrg-Ef1a-mCherry-IRES-Cre (Addgene,
127 55632-AAVrg) in the DLS at coordinates A/P: +0.7, M/L: ±2.4, D/V: −3.5 to express
128 GCaMP in AIC inputs to the DLS in a cre-dependent fashion. Bilateral 200 μm fiber optic
129 cannulas were also inserted into DLS at coordinates A/P: +0.7, M/L: ±2.4, D/V: −3.5.
130 The fiber optic cannulas were secured to the skull using OptiBond Universal etchant
131 (Henry Schein, Melville, NY) followed by Tetric EvoFlow light-cured, nano-optimized
132 flowable composite (Henry Schein, Melville, NY) and the skin was closed over the top of
133 the probe using Vetbond tissue adhesive (3M, Saint Paul, MN).

134 ***Drinking in the Dark***

135 The DID paradigm was based on the original DID procedure with two modifications
136 (Thiele and Navarro 2014). First, there were four 2 hr DID sessions (Monday–Thursday)
137 and one 4 hr DID session (Friday) and second, all DID sessions were performed out of
138 a single bottle of water or alcohol (20% v/v in water) via lickometers (described below)
139 inserted into the cage at the beginning of the DID session, which were removed at the

end of the DID session. Mice had *ab libitum* access to their standard water bottles at all other times.

To summarize the performed procedures, after animals recovered from surgery, they were singly housed and allowed to acclimate in a reverse 12 hr dark/light cycle (lights off at 06:00 hr) for 1 week. Wire feeding racks were removed from the cage and animals were floor fed to reduce damage to fiber optic probes protruding from their skulls. Three hours into the dark cycle (09:00 hr) animals were transferred to a behavior room, covered with blankets to avoid light exposure, and the homecage water bottle was removed from the cage. The lickometer was inserted into the cage after the homecage water bottle was weighed to calculate the inter-session water intake. Animals stayed in their own home cages for DID, but the lids were replaced with a clear cage top to allow for two down video recording of DID sessions.

Following the completion of 2- or 4-hr access, the lickometers were removed and the fluid bottles were weighed immediately after the session. Grams per kg (g/kg) of water and alcohol were computed from the difference in bottle weight and the density of water or 20% alcohol in water. The original cage tops were replaced, and animals were covered and transported back to their animal facility housing room. Mice were weighed post-DID session on Monday, Wednesday, and Friday (Tuesday and Thursday weights were equivalent to Monday and Wednesday, respectively). For Saturday and Sunday, the mice had no access to the lickometers as no procedures were performed. These 1-week repeating DID cycles are referred to as ‘Drinking Weeks’.

In-Vivo Fiber Photometry

Fiber photometry acquisition was performed with a Neurophotometrics fiber photometry system (FP3002, Neurophotometrics LTD, San Diego, CA). Briefly, this system utilized a pulsating 415-nm purple light LED as an isosbestic control and a 470-nm blue-light LED to excite GCaMP, each pulsating at 30 hertz with a power of 50 μW as measured out of the tip of each fiber optic cable. The fluorescence light path includes a dichroic mirror to pass emitted fluorescence to a complementary metal-oxide semiconductor camera (FLIR BlackFly, Goleta, CA) traveling through a dual branching 200 μm fiber optic patch cable (Doric Lenses, Québec, QC, Canada) allowing for the recording of isosbestic and

170 GCaMP fluorescence signals from both the left and right AIC inputs to the DLS,
171 simultaneously. Animals were plugged into patch cabling and then placed back in their
172 home cage for 5 minutes before lickometers were inserted and DID sessions started.
173 Fluorescence signals from the camera were captured with Bonsai (https://bonsai-
174 rx.org/docs), which also integrated and captured lickometer data via an Arduino Uno.

175 The fiber photometry signal was processed using a custom Python pipeline (code
176 available at: https://github.com/dlhagger). In summary, we removed the first 300 frames
177 from each recording and fit a biexponential decay function to the 415-nm isosbestic
178 channel for each recording, in each brain region. That fit was then robustly linearly
179 scaled using a RANdom Sample Consensus algorithm (RANSAC) to the 470-nm
180 GCaMP emission data. Finally, the 470-nm GCaMP emission data was lowpass filtered
181 at 6 Hz. Together these preprocessing steps control for photobleaching and motion
182 artifacts in the GCaMP recording. The acquired 470-nm GCaMP data was then divided
183 by the scaled 415-nm isosbestic control fit to compute a corrected observed
184 fluorescence value, or ΔF/F. For each recording, and each brain region, the process
185 was repeated, removing recordings with poor biexponential decay fits, excessive motion
186 artifacts, and/or for recordings in which cabling disconnects or tangles occurred. In total,
187 820 recordings were acquired and 36 were excluded from the dataset for further
188 analysis. Left and right AIC input ΔF/Fs were then z-scored by session for comparison
189 of signals across fluids, sex, brain side lateralization, and time.

190 For peri-event analysis, the initiation of each drinking bout was defined by a 10 second
191 sliding recording window including the 5 seconds before the bottle contact and 5
192 seconds post bottle contact. All z-scored ΔF/F values from both left and right sides were
193 then aligned to the drink start in this window.

194 ***Histology***

195 Animals were anesthetized with isoflurane and trans-cardially perfused with 15 ml of
196 ice-cold phosphate buffered saline (PBS) followed by 25 ml of ice-cold 4%
197 paraformaldehyde (PFA) in PBS. Animals were decapitated and the brain was extracted
198 and placed in 4% PFA for 24 hr. Brains were then transferred to 30% sucrose solution
199 until they sank after which they were sectioned on a vibratome at a section thickness of

200 50 μm. Brain sections were mounted in serial order on glass microscope slides and
201 stained with 4′,6-diamidino-2-phenylindole to visualize nuclei. Fluorescent images were
202 captured on a BZ-X810 fluorescent microscope (Keyence, Itasca, IL) using ×4 and ×20
203 air objectives. Injection site, viral expression, and the location of optogenetic probe
204 implantations were determined from matching images to the Reference Allen Mouse
205 Brain Atlas. Animals that did not have viral expression in the brain regions of interest
206 and/or did not have fiber optic cannula probe placements within the brain region of
207 interest as confirmed by histology were excluded from the study.

208 ***Lickometers***

209 All alcohol and water drinking experiments were performed using custom-built
210 homecage fluid monitors (i.e. 'lickometers') that were constructed with the following
211 modifications (Godynyuk, Bluitt et al. 2019). Liquid monitoring was constantly sampled
212 as a function of the state (open vs. closed) of an infrared beam directly in front of the
213 fluid bottle valve, and data was written to device memory every 3 seconds. This 3
214 second window ensured drinking activity data reliably saved to the hardware. Therefore,
215 any tube interaction within a 3 second window (defined as a drink) was recorded as the
216 total number of beam breaks (defined as events) for the total duration that the beam
217 was broken (defined as event duration) within that time window.

218 The lickometers can hold two bottles, although we only used one for each device during
219 these experiments. We randomized the bottle side location across animals and found
220 no effect on drinking, thus data are presented collapsed on bottle side.

221 Lickometer data was cleaned by fitting a linear model comparing the number of events
222 by the event duration within each bout for every DID session performed by each animal.
223 Events that had a residual value of greater than or less than 3 from model fit were
224 removed. This cleaning procedure removed events that were due to slow leaks (a new
225 tube was used if a leak was detected for the next DID session) or chews on the bottles
226 (Grecco, Haggerty et al. 2022, Haggerty, Munoz et al. 2022). Once raw lickometer data
227 were cleaned, no additional outliers were removed when computing events, event
228 durations, drinks, and/or any other microstructure elements.

For *in-vivo* fiber photometry experiments that utilized lickometers for time-resolving drinking behaviors with calcium imaging data, the lickometer's state changes triggered TTL outputs. 5V TTL signals were read using digital I/O pins on an Arduino Uno board flashed with the firmata firmware. The Arduino Uno's clock was synchronized to the fiber photometry acquisition software, so timestamps could be aligned to photometry data during data analysis with precise time resolution.

Microstructure feature analyses

Using events, event duration, drinks, and the timestamps when these events occurred during the DID session, we calculated other drinking features such as latency to drink (time to first bream break after session initiation) and mean inter-drink interval time per session (the mean time between drinks within each DID session). We also calculated features for events in the first 30 min of each DID session as a measure of front-loading behavior.

Modeling and statistics

Sample sizes for all experiments were determined based on our previously published experimental findings for electrophysiology and *in-vivo* behavioral assays such as DID (Munoz, Fritz et al. 2018, Haggerty, Munoz et al. 2022).

Data preprocessing and machine learning modeling utilized SciPy (Virtanen, Gommers et al. 2020), Statsmodels (Seabold and Perktold 2010), Scikit-learn (Pedregosa, Varoquaux et al. 2011), and TensorFlow (Abadi, Barham et al. 2016). Statistical analyses were performed using pingouin (V0.5.4, (Vallat 2018)). Data visualization used matplotlib (Hunter 2007) and seaborn (Waskom 2021) libraries. For time series and repeated measures, we used two-, three, or four-way mixed or repeated measures ANOVAs where appropriate, which represented time (session or week) as the repeated, within-subject variable, and the factor (fluid type, viral expression, bottle side, sex, etc.) as the between-subjects factor. All mixed ANOVA data were tested to see if variances between factors were equal and normal using the Levene test. For one-way non-normal ANOVAs, we used Welch ANOVAs. If there was a main effect for factor, we used pairwise t-tests to determine post hoc significance and p-values were Sidak corrected. For correlations between two variables, we tested multivariate normality using the

Henze-Zirkler test. If samples were normal, we used a Pearson's correlation to report r and p-values. If samples failed normality testing, we used a Shepherd pi correlation that returned the Spearman correlation after removing bi-variate outliers. To test for group differences in correlations that were statistically significant, we used an analysis of covariance (ANCOVA) where the covariate factor was sex. For tests of two factors, we tested for sample normality across factors using the Shapiro-Wilk omnibus test. For normal samples, we used Welch two-tailed t-tests to correct for unequal sample sizes. For samples that failed normality testing, we used the Mann-Whitney U test. All significance thresholds were placed at $p<0.05$ and all data and model fits are shown as mean ± standard error (68% confidence interval) of the mean (SEM) and/or by scatter plot with means and error bars indicating the SEM.

Results

Sex-dependent differences in water and alcohol Drinking in the Dark

We isolated AIC→DLS circuitry by injecting an anterograde adeno-associated virus (AAV) into the AIC encoding a cre-dependent genetically encoded calcium indicator (GCaMP) and a retrograde AAV to express cre, a recombinase enzyme, in the DLS and implanted bilateral optic cannulas in the DLS to visualize and record calcium activity in synaptic inputs that arise from AIC projections to the DLS in both male and female mice **(Figure 1a)**. For all viral and fiber placements please see **Figure 1 – Figure Supplement 1**.

Animals then underwent 6 weeks of the Drinking in the Dark (DID) paradigm where they had 0, 2, or 4 hours of access to water each day for 3 weeks, and then were transitioned to alcohol access for an additional 3 weeks **(Figure 1b)**. For DID sessions in the first 3 weeks, animals achieved stable levels of water intake across 15 water DID sessions, and there were no sex differences between male and female water drinking **(Figure 1c-d)**. By averaging water intakes by week, a clearer understanding of weekly water intakes can be computed with no noted water intake differences across week or by sex **(Figure 1e-f)**. During drinking weeks 4 to 6, when animals were transitioned from water to alcohol intake, mice reliably consumed binge-like levels of alcohol during the 4-hour sessions, which correlated with pharmacologically relevant levels of intake as

289 based on previous experiments in our laboratory using identical drinking measures
290 **(Figure 1g)** (Haggerty, Munoz et al. 2022). We failed to find differences in alcohol intake
291 between males and females across all DID sessions in this paradigm **(Figure 1h)**.
292 Nonetheless, when analyzing alcohol consumption by week, for both sexes, there was a
293 greater amount of alcohol drank during week 4 in comparison to week 5 **(Figure 1i)**.
294 This could be due to the transition from water to alcohol, in which the total fluid volume
295 consumed during water sessions is larger than alcohol sessions and may be supported
296 by the decreasing levels of alcohol intake seen in early alcohol DID sessions 16-19 as
297 animals adapt to consuming a new fluid type **(Figure 1h)**. By week, both male and
298 female animals experienced this decrease in alcohol intake in week 5 and 6 as
299 compared to week 4 of DID, but there were no sex differences or interactions between
300 sex and drinking week **(Figure 1j)**. Ultimately, both sexes consume binge-like levels of
301 alcohol, and in relation to the measured calcium activity at AIC inputs into the DLS
302 presented below, one can be confident that differences in these signals are not a
303 function of the total alcohol intake by sex.

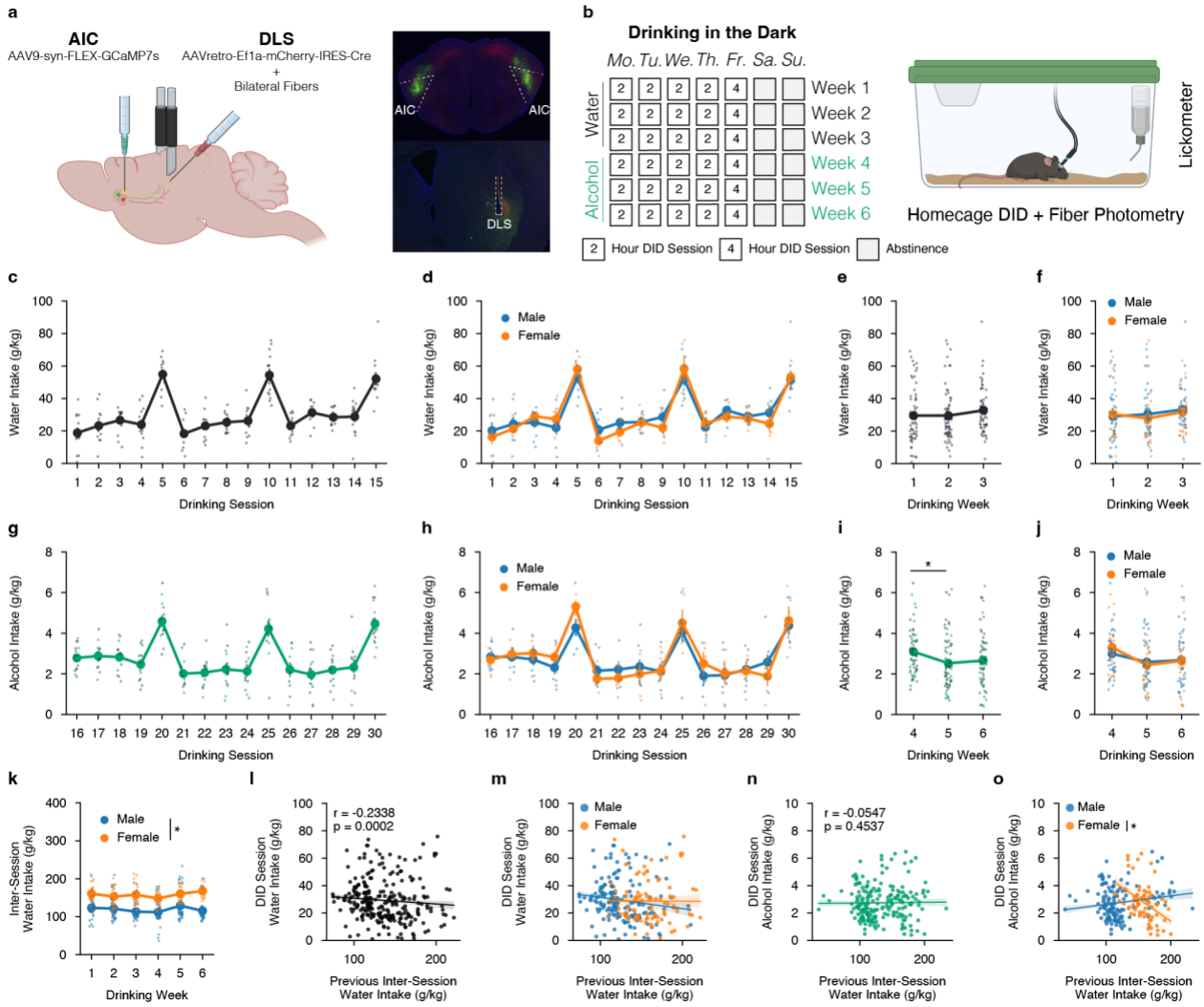

Figure 1: Sex-dependent differences in water and alcohol Drinking in the Dark (DID) (a) Representation of viral strategy and expression to record presynaptic calcium activity of AIC inputs within the DLS. **(b)** Schematic of Drinking in the Dark (DID) protocol. **(c)** Group and individual animals' water consumption by DID session (n = 14 animals). **(d)** Group and individual animals' water consumption by DID session and by sex (mixed ANOVA, Sex $F_{(1,12)} = 0.1032$, $p = 0.7535$; male n = 9, female n = 5). **(e)** Group and individual animals' water consumption by DID week (rmANOVA, Week $F_{(2,26)} = 2.4712$, $p = 0.1041$). **(f)** Group and individual animals' water consumption by DID week and by sex (mixed ANOVA, Sex $F_{(1,7)} = 0.1032$, $p = 0.7535$; male n = 9, female n = 5). **(g)** Group and individual animals' alcohol consumption by DID session (n = 14 animals). **(h)** Group and individual animals' alcohol consumption by DID session and by sex (mixed ANOVA, Sex $F_{(1,7)} = 0.4714$, $p = 0.5144$; male n = 9, female n = 5). **(i)** Group and individual animals' alcohol consumption by DID week (rmANOVA, Week $F_{(2,26)} = 7.8861$, $p = 0.0021$; Week 4 to Week 5, $p = 0.0012$; male n = 9, female n = 5). **(j)** Group and individual animals' alcohol consumption by DID week and by sex (mixed ANOVA, Sex $F_{(1,7)} = 0.4714$, $p = 0.5144$; male n = 9, female n = 5). **(k)** Group and individual animals' inter-session water consumption by DID week and by sex (mixed ANOVA, Sex $F_{(1,12)} = 13.5883$, $p = 0.0031$; male n = 9, female n = 5). **(l)** Previous inter-session water intakes negatively correlate with next DID session water intake (Shepherd's pi correlation, $r = -0.2383$, $p = 0.0002$). **(m)** Previous inter-session water intakes do not correlate with next DID session water intake by sex (ANCOVA, Sex $F(1,257) = 0.3048$, $p = 0.5814$; male n = 9, female n = 5). **(n)** Previous inter-session water intakes do not correlate with next DID session alcohol intake (Shepherd's pi correlation, $r = -0.0547$, $p = 0.4537$). **(o)** Previous inter-

325 session water intakes do not correlate with next DID session alcohol intake by sex (ANCOVA, Sex
326 $F_{(1,315)}$ = 0.0101, p = 0.9201; male n = 9, female n = 5), but when a priori splitting by sex females, but
327 not males, future alcohol intakes are negatively correlated with increasing amounts of inter-session
328 water intakes (males only r = 0.1554, p = 0.0916; females only r = -0.4441, p = 0.0002).

329 The amount of water intake between DID sessions was also measured daily using the
330 home cage water bottle. Interestingly, females consumed more water between both
331 water and alcohol DID sessions across all 6 weeks compared to males **(Figure 1k)**.
332 Previous inter-session DID water intakes were also correlated to the next DID session
333 intake to see if the amount of water consumed before any water DID session had any
334 influence on the amount of water consumed during the upcoming DID session. We
335 found a modest, yet statistically significant negative correlation **(Figure 1l)**. This
336 suggests that increased water intake, a proxy measurement for a quenched thirst state,
337 being achieved before a water DID sessions can predict lower levels of water consumed
338 during the DID session itself. We found no sex differences in this correlation between
339 males and females **(Figure 1m)**. Similarly, we questioned if inter-session water intakes
340 influenced future alcohol DID intakes, which we did not find to be true when looking at
341 the data blind to sex **(Figure 1n)**. Yet, the patterning between males and females for
342 thirst states looks strikingly different. While we did not find a statistically significant
343 difference using sex as a grouping variable in a co-variate analysis of variance
344 (ANCOVA) to determine if the slopes of the regression fits were statistically different, if
345 one *a priori* separates sex and then runs a regression, the correlation for male
346 intersession water intakes predicting alcohol DID intakes is not significant (p = 0.0916),
347 whereas increasing female intersession water intake is negatively and significantly
348 correlated (p = 0.0002, r = -0.4441) with lower alcohol DID intakes **(Figure 1o)**.
349 Together, this may suggest that the elevated inter-session DID water intakes correlate
350 with decreased levels of alcohol intake during DID sessions for females and may offer
351 another explanation for why females and males binge drank similar levels of alcohol in
352 this behavioral paradigm.

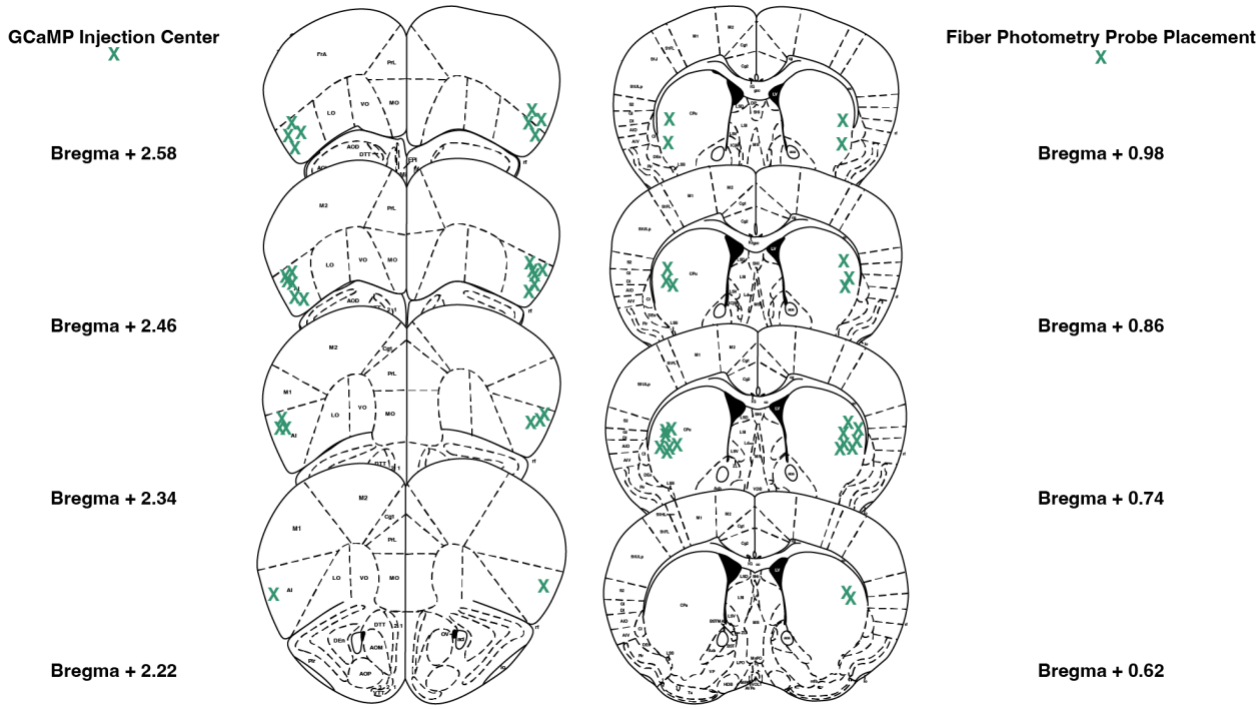

Figure 1 - Figure Supplement 1: Locations of anterior insular cortex (AIC) injections and dorsolateral striatum (DLS) injections and fiber optic cannula placements. Bilateral injection centers of AAV-FLEX-GCaMP in the AIC and bilateral injection centers of AAVrg-cre-mCherry and fiber optic cannula placements as verified by histology (male: n = 9 animals; female n = 5 animals).

Sex-dependent differences in water and alcohol drinking mechanics

We also aimed to understand how well animals' intakes correlated with both water and alcohol drinking microstructure measurements made directly from the lickometer in a sex-dependent manner. First, we plotted drinking events, drinking event duration, and number of drinks (i.e. cumulative drinking events that occurred in a 3 second window) and correlated them to water intake across all DID water sessions.

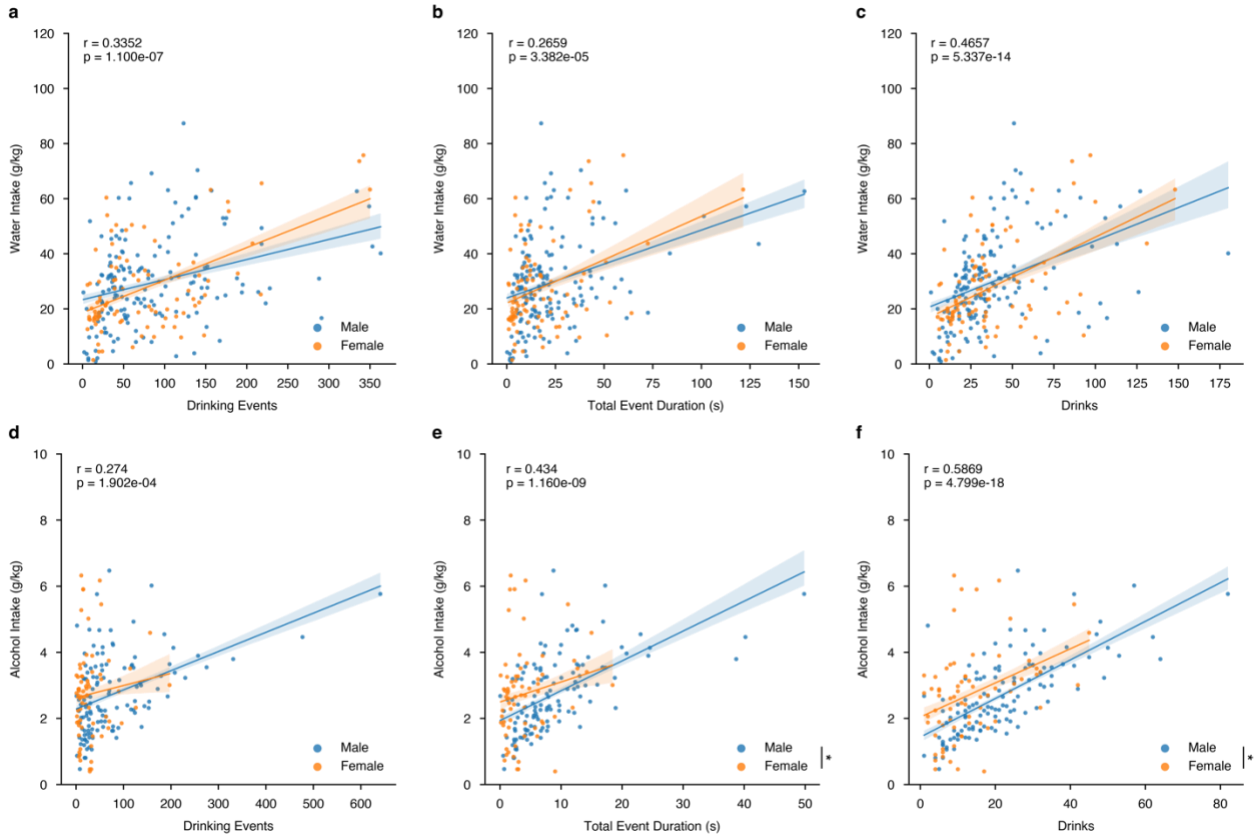

Figure 2 – Figure Supplement 1: Microstructure features measured from lickometers correlate with alcohol and water intakes in a sex-dependent manner. **(a)** Water events (Shepherd's pi correlation, r = 0.3352, p = 1.1e-07; ANCOVA, Sex $F_{(1, 252)}$ = 0.3203, p = 0.5719; male n = 9, female n = 5), **(b)** total event duration (Shepherd's pi correlation, r = 0.2726, p = 2.001e-05; ANCOVA, Sex $F_{(1, 252)}$ = 0.0757, p = 0.7834; male n = 9, female n = 5), and **(c)** drinks (Shepherd's pi correlation, r = 0.4622, p = 9.884e-14; ANCOVA, Sex $F_{(1, 252)}$ = 0.9928, p = 0.32; male n = 9, female n = 5) correlate with water intakes in a non sex-dependent manner. **(d)** Alcohol events (Shepherd's pi correlation, r = 0.274, p = 0.0001902; ANCOVA, Sex $F_{(1, 191)}$ = 2.13, p = 0.1461; male n = 9, female n = 5) correlate with alcohol intakes in a non-sex dependent manner. Yet, alcohol **(e)** event duration (Shepherd's pi correlation, r = 0.434, p = 1.16e-09; ANCOVA, Sex $F_{(1, 191)}$ = 5.689, p = 0.01805; male n = 9, female n = 5) and **(f)** drinks (Shepherd's pi correlation, r = 0.5869, p = 4.799e-18; ANCOVA, Sex $F_{(1, 191)}$ = 9.7152, p = 0.00211; male n = 9, female n = 5) correlate with alcohol intakes and females display a sex-dependent increase in intake for these metrics. Individual datapoints represent a microstructure feature and intake taken from a single DID session. Data were fit to a linear model represented by a line of best fit with shading indicating ± SEM. Axes histograms display distribution of microstructure features and intakes across all DID sessions.

For water events, event duration, and number of drinks, were all significantly correlated with intake and there were no differences in how male and female mice consumed water out of the lickometers across all DID water sessions **(Figure 2 – Figure**

Supplement 1a-c). Similarly, alcohol events, event duration, and number of drinks were all highly correlated to alcohol intake **(Figure 2 – Figure Supplement 1d-f)**. For drinking events, there were no sex differences, yet for the alcohol event duration and number of alcohol drinks, female mice showed an increased correlation with alcohol intake at lower event numbers and drinks compared to males, suggesting they might be more efficient drinkers, such that efficiency measures the ability to consume more alcohol in a single drinking interaction compared to males **(Figure 2 – Figure Supplement 1f)**.

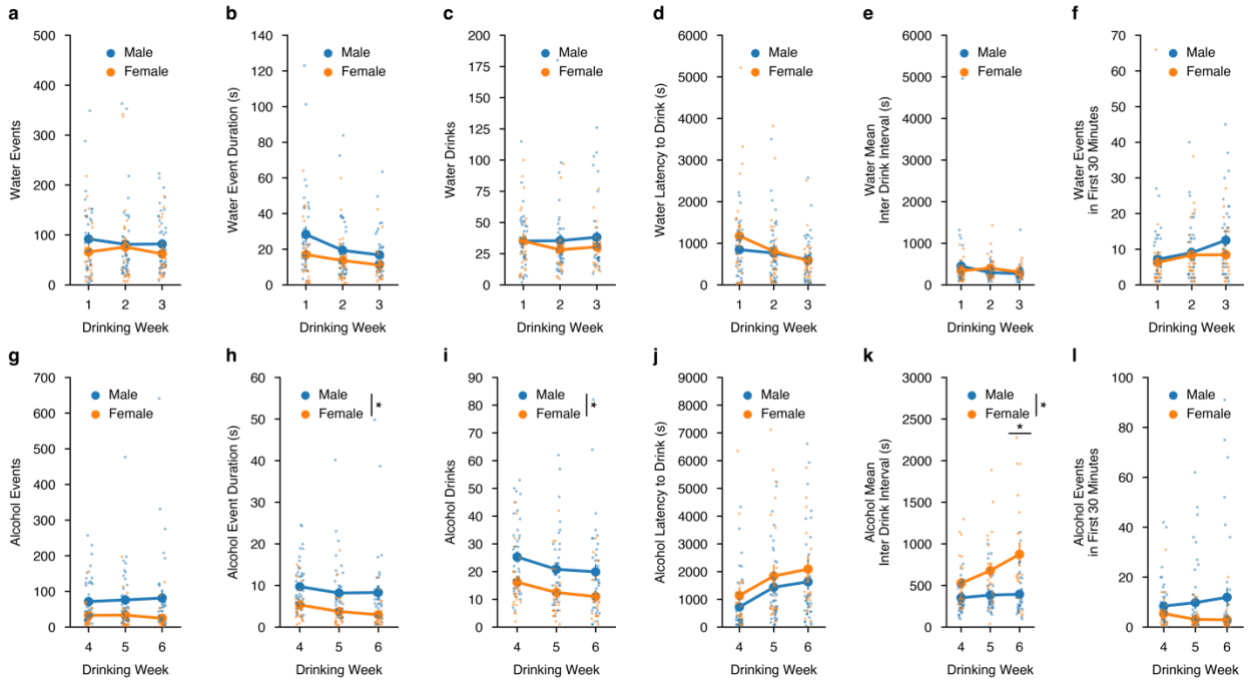

Figure 2: Alterations in drinking microstructure represent different strategies used to consume similar levels of alcohol, but not water intake in a sex-dependent manner. Water **(a)** events (mixed ANOVA, Sex $F_{(1,11)} = 0.6164$, $p = 0.4490$; male n = 9, female n = 5), **(b)** total event duration (mixed ANOVA, Sex $F_{(1,11)} = 1.422$, $p = 0.2582$; male n = 9, female n = 5), **(c)** drinks (mixed ANOVA, Sex $F_{(1,11)} = 0.3957$, $p = 0.5422$; male n = 9, female n = 5), **(d)** latency to drink (mixed ANOVA, Sex $F_{(1,11)} = 0.3911$, $p = 0.5746$; male n = 9, female n = 5) **(e)**, mean inter-drink interval (mixed ANOVA, Sex $F_{(1,11)} = 0.0339$, $p = 0.8572$; male n = 9, female n = 5), and **(f)** events in the first 30 minutes of a DID session (mixed ANOVA, Sex $F_{(1,11)} = 0.538$, $p = 0.4786$; male n = 9, female n = 5) do not differ by sex across drinking week. Alcohol **(g)** events do not differ by sex across week (mixed ANOVA, Sex $F_{(1,12)} = 3.183$, $p = 0.0997$; male n = 9, female n = 5), but alcohol **(h)** event duration (mixed ANOVA, Sex $F_{(1,12)} = 7.286$, $p = 0.0193$; male n = 9, female n = 5), and **(i)** drinks are decreased in female compared to male binge alcohol drinkers (mixed ANOVA, Sex $F_{(1,12)} = 6.681$, $p = 0.0239$; male n = 9, female n = 5). There were no sex differences in alcohol **(j)** latency to drink (mixed ANOVA, Sex $F_{(1,12)} = 1.914$, $p = 0.1917$; male n = 9, female n = 5) **(k)**, but alcohol mean inter-drink interval is increased in females compared to males (mixed ANOVA, Sex x Week $F_{(2,24)} = 3.623$, $p = 0.0422$; Week 6 $t_{(6.81)} = 3.623$, $p = 0.01882$; male n = 9, female n = 5). There are no sex-

412 dependent changes in **(l)** events in the first 30 minutes of an alcohol DID session by week (mixed
413 ANOVA, Sex $F_{(1,12)} = 1.972$, $p = 0.1856$; male n = 9, female n = 5).

414 We also wanted to see how these microstructure analyses were altered across time
415 between sex. For water intake, across DID weeks 1-3, there were no sex differences in
416 the number of events, event durations, water events, the latency to drink water, the
417 mean inter-drink interval between water events, nor differences in front loading behavior
418 for water intake **(Figure 2a-f)**. For alcohol intake, across DID weeks 4-6 there were no
419 sex differences for the number of alcohol events, but females did have a decreased
420 time for alcohol event durations and number of alcohol drinks compared to males
421 **(Figure 2g-i)**. These findings across time further support that females may be more
422 efficient in consuming alcohol, such that it requires less time and drinks to reach similar
423 levels of alcohol intake that males achieve. Females and males displayed the same
424 latency to drink alcohol across time, but as DID weeks progressed, females displayed
425 an increased inter-drink interval **(Figure 2j-k)**. Finally, both males and females displayed
426 similar levels of front-loading behavior for alcohol **(Figure 2l)**. Together, these data
427 suggest that when alcohol intake levels are similar between males and females, the way
428 in which they achieve those intakes may be dissimilar in both the manner in how
429 females consume alcohol and how those differences in consumption evolve across
430 time.

431 ***Calcium dynamics of AIC inputs into the DLS during drinking bouts***

432 To visualize changes in calcium dynamics at the AIC presynaptic inputs to both the left
433 and right DLS, we aligned the changes in calcium fluorescence to the beginning of
434 water and alcohol drinking events, creating a 10 second window with 5 seconds before
435 the initiation of the drinking event and 5 seconds after.

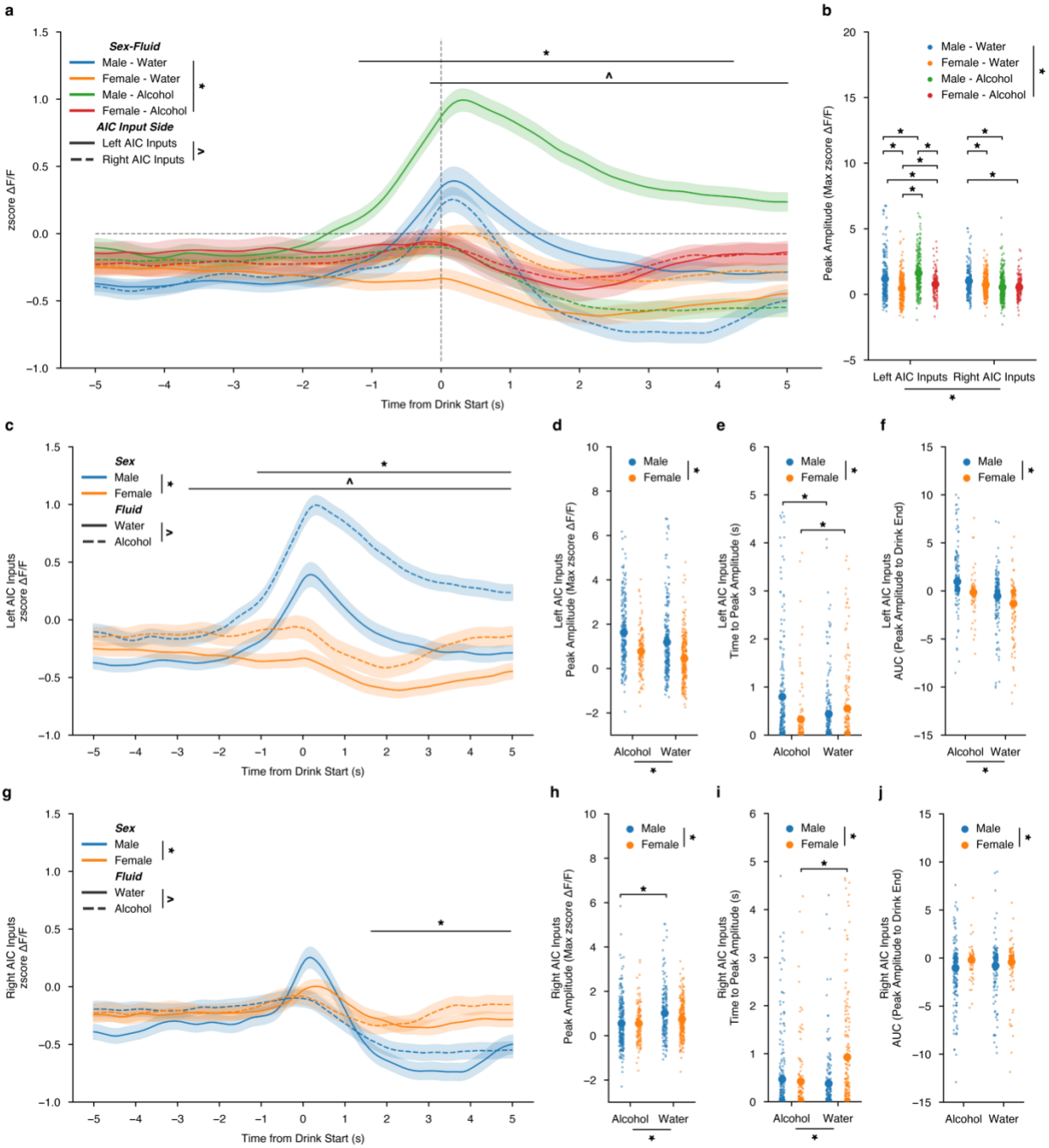

Figure 3: Sex-dependent calcium dynamics of AIC inputs into the left and right DLS during water and drinking bouts. (a) AIC inputs to the DLS are most strongly engaged by alcohol at AIC inputs into the left DLS (ANOVA, Sex x Fluid x Time x Input Side $F_{(149,200.7)} = 1.383$, $p = 0.001383$; * = Time from Drink Start x AIC Input Side, -0.0369128 (s) – 5 (s), $p < 0.05$; ^ = Time from Drink Start x Sex-Fluid, -1.308725 (s) – 4.95733 (s), $p < 0.05$) and **(b)** peak amplitudes ΔF/F changes are strongly associated with changes in AIC inputs to the left DLS than with the right DLS (ANOVA, Sex x Fluid x Input Side $F_{(3,122.6)} = 31.15$, $p = 1.298e\text{-}19$). **(c)** For left AIC inputs into the DLS, there were both sex and fluid interactions by time for changes in ΔF/F (ANOVA, Sex x Fluid x Time $F_{(149,221.9)} = 1.404$, $p = 8.419e\text{-}4$; * = Time from Drink Start x Sex, -1.107383 (s) – 5 (s), $p < 0.05$; ^ = Time from Drink Start x Fluid, -2.181208 (s) – 5 (s), $p < 0.05$) and **(d)** increases in peak amplitude for ΔF/F for alcohol

compared to water were observed, but no interaction was present between sex and fluid (ANOVA, Fluid $F_{(1,32.45)}$ = 19.46, p = 1.152e-5; Sex $F_{(1,132.2)}$ = 79.27, p = 2.919e-18). **(e)** Time to peak values for males increased due to alcohol exposure, yet the opposite occurred for females (ANOVA, Sex x Fluid $F_{(1,14.25)}$ = 19.44, p = 0.000012; paired t-test, males $t_{(375.5)}$ = 4.0864, p = 0.000107; paired t-test, females, $t_{(280.5)}$ = -2.532 p = 0.02361). **(f)** Left AUC were increased in males in comparison to females, but no interaction was present between sex and fluid (ANOVA, Fluid $F_{(1,332.3)}$ = 56.58, p = 1.652e-13; Sex $F_{(1,149.8)}$ = 25.51, p = 5.613e-7). **(g)** For right AIC inputs into the DLS, there were both sex by time and fluid by time for changes in ΔF/F, but no three-way interaction (ANOVA, Sex x Time $F_{(149,\ 772.6)}$ = 5.881, p = 6.559e-103; ^ = Time from Drink Start x Sex, -1.778523 (s) – 5 (s), $p < 0.05$; Fluid x Time $F_{(149,340.7)}$ = 2.594, p = 5.977e-23). **(h)** Decreases in peak amplitude ΔF/F for alcohol compared to water were observed for males, but not females (ANOVA, Sex x Fluid $F_{(1,3.652)}$ = 3.925, p = 0.04787; paired t-test, males $t_{(407.1)}$ = 4.490, p = 0.000009; paired t-test, females, $t_{(271.9)}$ = -2.248 p = 0.05015). **(i)** For females, time to peak decreased when transitioning from water to alcohol exposure, but there was no effect in males (ANOVA, Sex x Fluid $F_{(1,15.02)}$ = 20.99, p = 0.000005; paired t-test, males $t_{(410)}$ = 1.288, p = 0.1985; paired t-test, females, $t_{(289.6)}$ = - 4.558 p = 0.000008). **(j)** For AUC, there was only a main effect of sex, with females displaying larger AUCs across both water and alcohol compared to males (ANOVA, Sex x Fluid $F_{(1,15.02)}$ = 20.99, p = 0.000005). GCaMP activity is aligned to the initiation of the water drinking bout with 5 seconds before and 5 seconds after the bout plotted. Solid lines represent means, and shading or error bars represent the standard error of the mean.

First, to summarize the differences between calcium activity at left and right inputs to the DLS, we averaged all z-scored water and alcohol drinking sessions' calcium activity and compared them for sex, fluid, lateralization, and time differences. Altogether, it showed that drinking behaviors are largely encoded by male AIC inputs into the left DLS, with alcohol displaying the largest change in magnitude for ΔF/F both across time (**Figure 3a**). We also show robust differences in AIC signals that are sex, fluid, and lateralization dependent across time during the drink window (**Figure 3a**). When analyzing peak amplitude of the calcium signals, we also find that alcohol left male AIC inputs show the largest magnitude, and water left AIC inputs the second largest when time locked to drinking events **(Figure 3b)**. Since AIC inputs into the DLS display strong lateralized effects, we split the data by left and right AIC inputs into the DLS to zoom in on the sex and fluid comparisons occurring at each input. By looking at all AIC inputs into the left DLS by sex and fluid, calcium activity is increased for alcohol compared to water across time for both sexes, but especially in males **(Figure 3c)**. More detailed analyses of the dynamics of the calcium signals also displayed both sex and fluid differences for the peak amplitude of the calcium signal where males show increased peak amplitudes for both water and alcohol compared to females (**Figure 3d**). We also measured the time to the maximum calcium signal, time to peak, during the drinking event to determine if alcohol or sex displayed a time-dependent shift in the on-kinetics of the calcium signal.

485 Interestingly, a sex by fluid interaction shows that for males, binge alcohol consumption,
486 compared to water, increases the amount of time that it takes for the peak calcium
487 signal to occur (**Figure 3e**). Whereas in females, binge alcohol consumption, compared
488 to water, decreases the time to peak **(Figure 3e)**. Finally, we measured the area under
489 the curve using ΔF/F values from the time when the peak ΔF/F value occurred to the
490 time when the end of the drink occurred to assess the decay kinetics of the calcium
491 signal. For left AIC inputs, the AUC measurements also showed both sex and fluid
492 differences, such that the AUC for both water and alcohol measures were increased
493 compared to females, suggesting that the calcium signals were larger and remained
494 elevated for longer after the peak occurred **(Figure 3f).**

495 For AIC inputs into the right DLS by sex and fluid across time, compared to the left AIC
496 inputs, these findings are reversed, such that a decrease calcium for alcohol compared
497 to water is present, especially in males, and that the sex differences, regardless of the
498 fluid consumed, are mainly driven by differences in the off-kinetics of the calcium
499 dynamics. **(Figure 3g)**. In more detail, an interaction between sex and fluid for peak
500 amplitude shows that males decrease their peak amplitude calcium signals as they
501 transition to binge alcohol consumption **(Figure 3h)**. For time to peak, like left AIC
502 inputs, females see a decrease in time to peak as they switch from water to binge
503 alcohol drinking, yet there is no change in males **(Figure 3i)**. Finally, there was only a
504 sex dependent decrease in males compared to females for AUC, regardless of fluid
505 **(Figure 3j)**. In summary, two main findings are apparent, such that 1) for left AIC inputs,
506 regardless of sex, alcohol increases calcium activity compared to water during drinking
507 events and for right AIC inputs, alcohol decreases calcium activity compared to water
508 drinking events, and 2) that male calcium dynamics at both left and right AIC inputs are
509 more strongly altered by alcohol exposure than female calcium dynamics. Together, we
510 also observed a net shift towards increased engagement of AIC inputs into the left DLS
511 during transition from water to binge alcohol drinking in males, but not females, is
512 achieved via both increasing AIC engagement to the left DLS and decreasing AIC
513 engagement to the right DLS during drinking events.

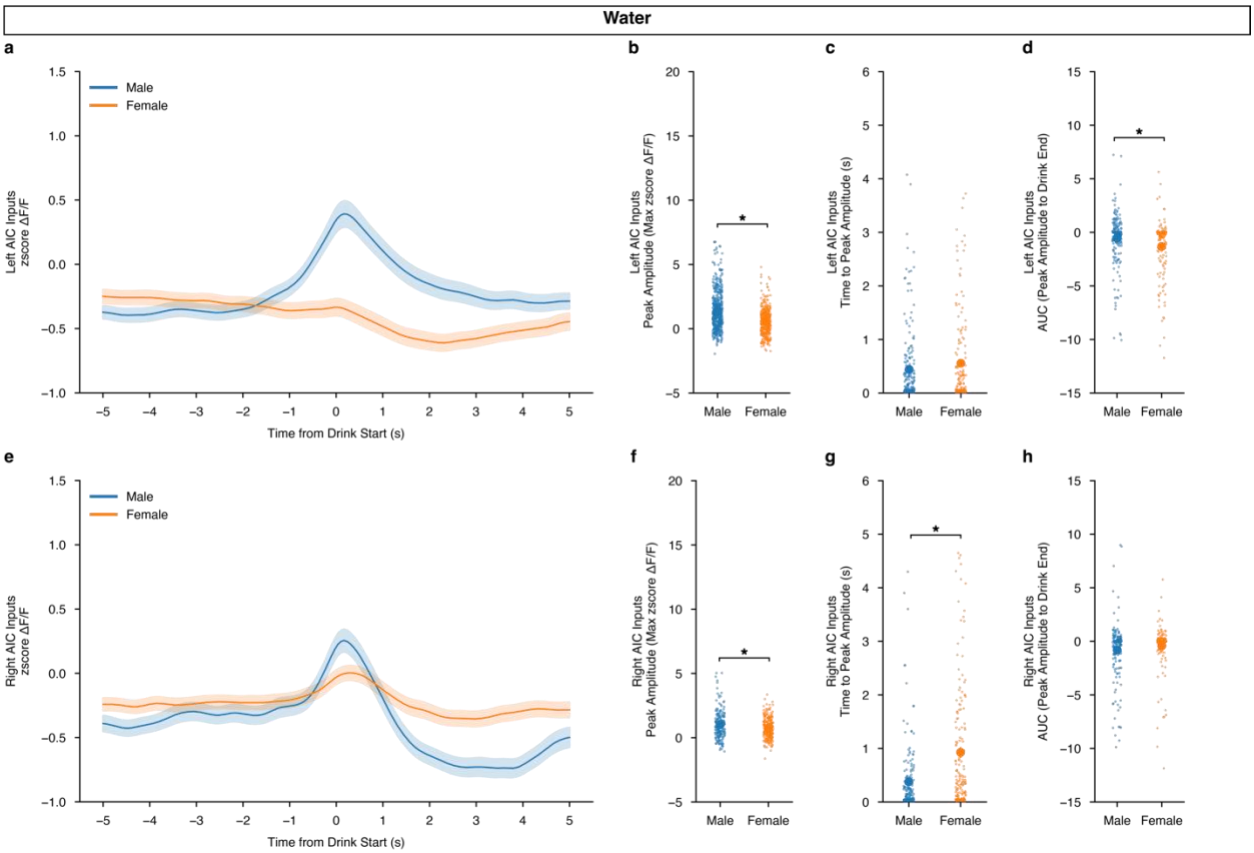

Figure 3 – Figure Supplement 1: Calcium dynamics of AIC inputs into the left and right DLS during water drinking. (a) Left AIC inputs to the DLS do not display a sex by time dependent change in ΔF/F (mixed ANOVA, Sex x Time $F_{(149,1341)}$ = 0.6601, p = 0.9993) **(b)** but for peak amplitude, males show larger maximum ΔF/F after water drinking events (MWU, U = 4465, p = 1.339e-8). **(c)** There were no differences in time to peak (MWU, U = 16410, p = 0.7269), **(d)** but the AUC for males was larger than females for left AIC inputs (MWU, U = 20100, p = 0.001031). **(e)** Right AIC inputs to the DLS also do not display a sex by time dependent change in ΔF/F (mixed ANOVA, Sex x Time $F_{(149,1192)}$ = 0.5882, p = 0.9996. **(f)** but like left AIC inputs, peak amplitudes in males were increased in males (MWU, U = 27902, p = 0.02137). **(g)** Female time to peak values also increased in comparison to males (MWU, U = 989, p = 5.238e-8), **(h)** but no changes in AUC were observed by sex (MWU, U = 13242, p = 0.06568) GCaMP activity is aligned to the initiation of the water drinking bout with 5 seconds before and 5 seconds after the bout plotted. Solid lines represent means and shading or error bars represent the standard error of the mean.

Since we uncovered fluid effects for both left and right AIC inputs across the time from drink start, we wanted to further examine the sex effects observed and to understand how AIC inputs evolved across the drinking task within each fluid. To do this, we filtered the dataset presented in Figure 3 to include only water drinking events and then analyzed for sex differences. Looking at all water events, we failed to detect a sex difference for both left and right AIC inputs into the DLS across the time from drink start **(Figure 3 – Figure Supplement 1a & e)**. For left AIC inputs during water drinking, we did see an increase in peak amplitude, no change in time to peak amplitude, and an

increase in AUC for males compared to females **(Figure 3 – Figure Supplement1b-d)**. For right AIC inputs, similarly, an increase in peak amplitude was observed **(Figure 3-Figure Supplement 1f)**. Females also displayed an increased time to peak, but there was no sex effect for AUC **(Figure 3 – Figure Supplement 1g-h)**.

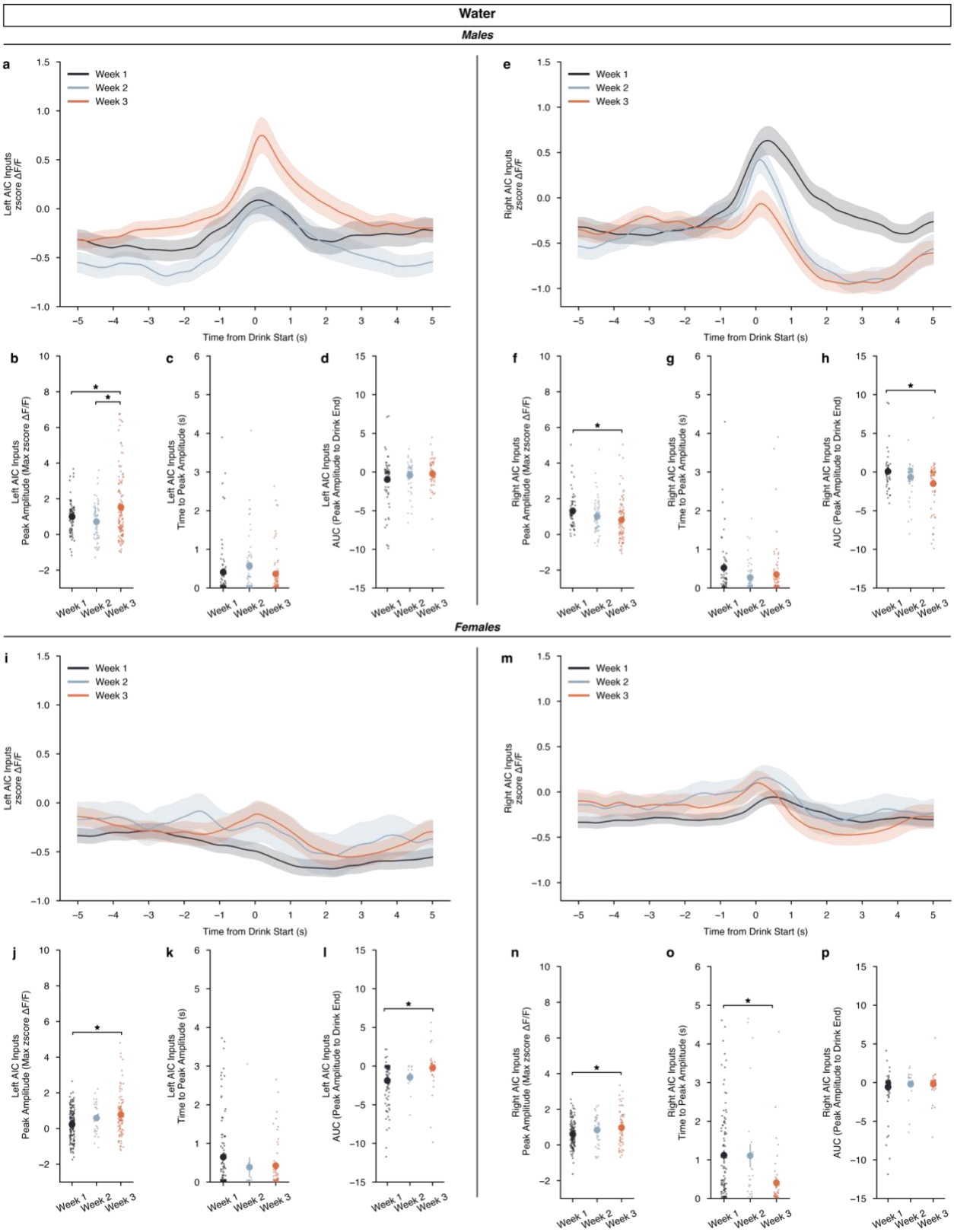

Figure 4: Calcium dynamics of AIC inputs into the left and right DLS across water drinking

weeks. (a) For males, left AIC inputs to the DLS do not display a by week dependent change in ΔF/F (rmANOVA, DID Week x Time from Drink $F_{(298,298)}$ = 0.6953 , p = 0.5575), but **(b)** peak amplitudes increased in the final week of water drinking compared to the first two (ANOVA, DID Week $F_{(2,163.8)}$ = 7.235 , p = 0.000975; Week 3 – Week 1, p = 0.02478; Week 3 – Week 2, p = 0.000557). Yet, no difference in **(c)** time to peak (ANOVA, DID Week $F_{(2,127.4)}$ = 1.556, p = 0.215) or **(d)** AUC were observed by week (ANOVA, DID Week $F_{(2,129.9)}$ = 1.405 , p = 0.2491) for male, left AIC inputs. **I** Right AIC inputs to the DLS did also not display a by week dependent change in ΔF/F (rmANOVA, DID Week x Time from Drink $F_{(298,596)}$ = 2.166 , p = 0.2743), but **(f)** a decrease in peak amplitudes in the final water drinking week was observed in comparison to the first week (ANOVA, DID Week $F_{(2,192)}$ = 3.5774, p = 0.02983; Week 3 – Week 1, p = 0.02206). **(g)** No change in time to peak was observed by week (ANOVA, DID Week $F_{(2,104.6)}$ = 2.139, p = 0.1229), but **(h)** a decrease in AUC was observed with the final week of water drinking displaying a deceased off-kinetic of the calcium signal in comparison to the initial drinking week (ANOVA, DID Week $F_{(2,113.9)}$ = 5.301, p = 0.006291; Week 3 – Week 1, p = 0.004061). **(i)** For females, left AIC inputs to the DLS do not display a by week dependent change in ΔF/F (rmANOVA, DID Week x Time from Drink $F_{(298,298)}$ = 1.308, p = 0.5817), but **(j)** like males, peak amplitudes increased in the final week of water drinking (ANOVA, DID Week $F_{(2,78.83)}$ = 7.529, p = 0.001017; Week 3 – Week 1, p = 0.00108). No difference in **(k)** time to peak (ANOVA, DID Week $F_{(2,30.37)}$ = 1.591, p = 0.2203) was observed, but **(l)** AUC increased in the final week of water drinking compared to the initial week (ANOVA, DID Week $F_{(2,34.22)}$ = 7.0389, p = 0.002751; Week 3 – Week 1, p = 0.000801). **(m)** Right AIC inputs to the DLS did also not display a by week dependent change in ΔF/F (rmANOVA, DID Week x Time from Drink $F_{(298,596)}$ = 1.022 , p = 0.4966), but **(n)** an increase in peak amplitudes in the final water drinking week was observed in comparison to the initial week (ANOVA, DID Week $F_{(2,93.65)}$ = 4.533, p = 0.01321; Week 3 – Week 1, p = 0.01778). **(o)** A decline in time to peak was observed in the final week of water drinking (ANOVA, DID Week $F_{(2,58.75)}$ = 10.26, p = 0.000151; Week 3 – Week 1, p = 0.00066), but **(p)** no change in AUC was observed by week (ANOVA, DID Week $F_{(2,64.13)}$ = 0.7386, p = 0.4818). GCaMP activity is aligned to the initiation of the water drinking bout with 5 seconds before and 5 seconds after the bout plotted. Solid lines represent means, and shading or error bars represent the standard error of the mean.

Additionally, observing how the development of water drinking, across weeks, altered calcium dynamics we found that for water drinking in males, there were no differences by DID week in either the left or right AIC inputs across time from drink starts **(Figure 4 1a & e)**. For left inputs in water-drinking males, we observed an increase in the peak amplitude in week 3 compared to weeks 1 and 2, but no change in time to peak or AUC measurements **(Figure 4b-d)**. For the right inputs in water-drinking males, we saw the opposite for peak amplitudes, a decrease in week 3 compared to week 1, no change in

time to peak, and a decrease in the AUC in week 3 compared to week 1 **(Figure 4f-h)**. For females, there were no differences by DID week in either the left or right AIC inputs across time from drink starts **(Figure 4j & m).** We see similar changes, such that left AIC inputs for water-drinking females also increase peak amplitude, with no change in time to peak by week, like left AIC inputs in water-drinking males **(Figure 4j-k)**. Although, increases in AUC are seen in week 3 compared to week 1 **(Figure 4l)**. For right AIC inputs we see an increase in peak amplitude in week 3 compared to week 1, with a decrease in time to peak, and no changes in AUC **(Figure 4n-p)**. Together, we see no effect across water drinking weeks when looking at the calcium signal in the entire water drinking window, and only small alterations in calcium signal when looking at specific parts (peak amplitude, time to peak, and AUC) of the calcium dynamics across sex. Generally, as the animals experience more water DID sessions, AIC inputs become more engaged during water drinking events as measured by increases in peak amplitude, with corresponding increases in AUC in some cases.

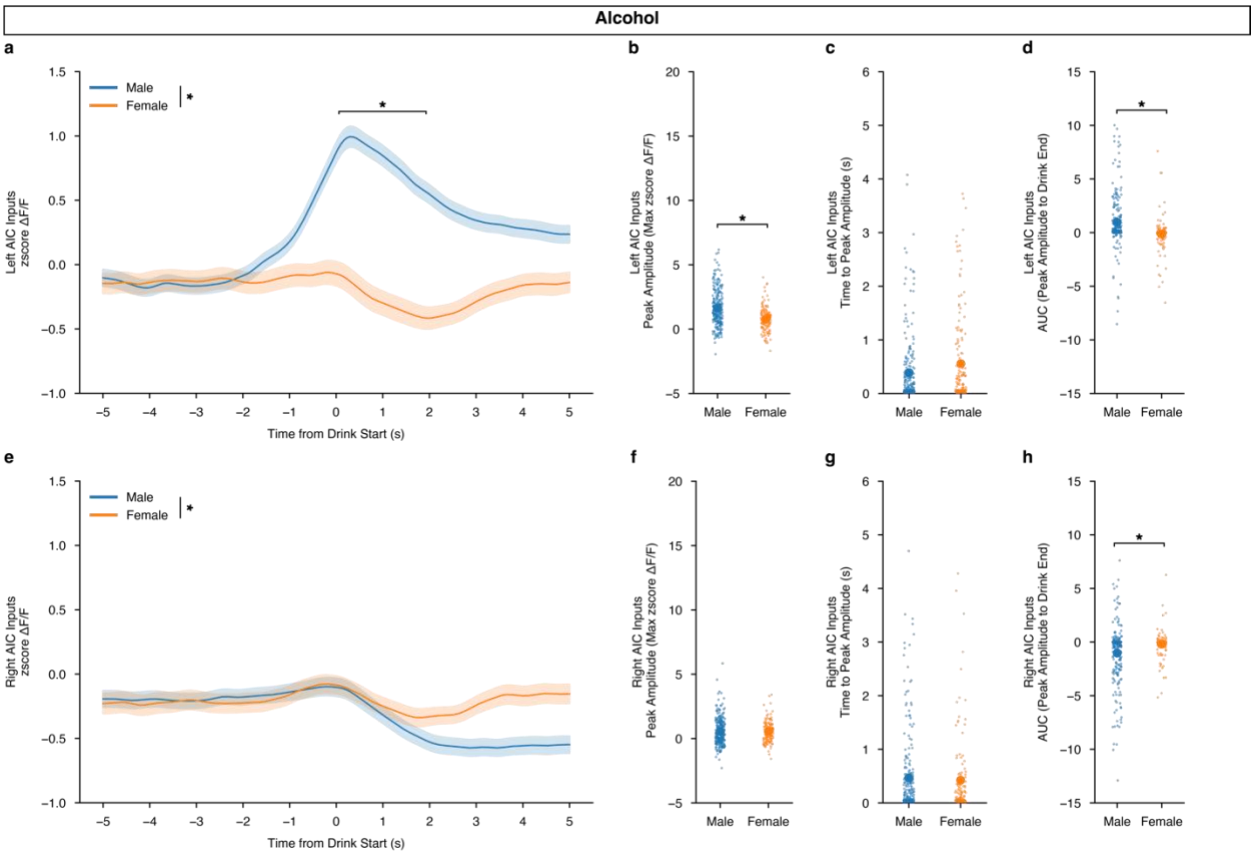

Figure 3 – Figure Supplement 2: Left AIC inputs into the DLS encode binge alcohol drinking in males, but not females. (a) Left AIC inputs to the DLS display an increase in sex by time dependent

change in ΔF/F, with males displaying an increased calcium signal after alcohol drinking initiation compared to (mixed ANOVA, Sex x Time $F_{(149,1788}$ = 3.125, p = 4.006e-29; Time from Drink Start, 0.0369128 (s) – 1.989866 (s), p <= 0.05) and **(b)** male peak amplitudes are increased compared to females (MWU, U = 22385, p = 2.379e-9). **(c)** There were no differences in time to peak (MWU, U = 18174.5, p = 0.2148), **(d)** but the AUC for males was larger than females for left AIC inputs during binge alcohol drinking (MWU, U = 19025, p = 1.281e-11). **(e)** Right AIC inputs to the DLS also display a sex by time dependent change in ΔF/F, but no post hoc significance for any individual timepoint was discovered (mixed ANOVA, Sex x Time $F_{(149,1788)}$ = 1.2821, p = 0.00151) **(f)** nor were right AIC peak amplitudes different by sex (MWU, U = 17217, p = 0.5484). **(g)** No change in time to peak values were observed (MWU, U = 16045, p = 0.8015), **(h)** but female AUC measurements were greater than males (MWU, U = 12561.5, p = 0.001092). GCaMP activity is aligned to the initiation of the water drinking bout with 5 seconds before and 5 seconds after the bout plotted. Solid lines represent means, and shading or error bars represent the standard error of the mean.

When performing the same analysis, i.e. filtering the dataset presented in Figure 3, but for only binge alcohol drinking sessions, we see that for left AIC inputs, we show a strong sex dependent engagement from approximately the time to peak for about two seconds **(Figure 3 – Figure Supplement 2a)**. As a result, an increase in peak amplitude and AUC is also observed, with no change in time to peak across sex **(Figure 3 – Figure Supplement 2b-d)**. For right AIC inputs, we observed no change in calcium signal across time from drink start, no change in peak amplitude, nor any change in time to peak during binge alcohol consumption (**Figure 3 – Figure Supplement 2e-g**), but we did observe a slight decrease in AUC that represents the decreased signal seen in the off-kinetics in males compared to females (**Figure 3 – Figure Supplement 2h**). These data further detail how left AIC inputs strongly encode binge alcohol consumption in male, but not female mice.

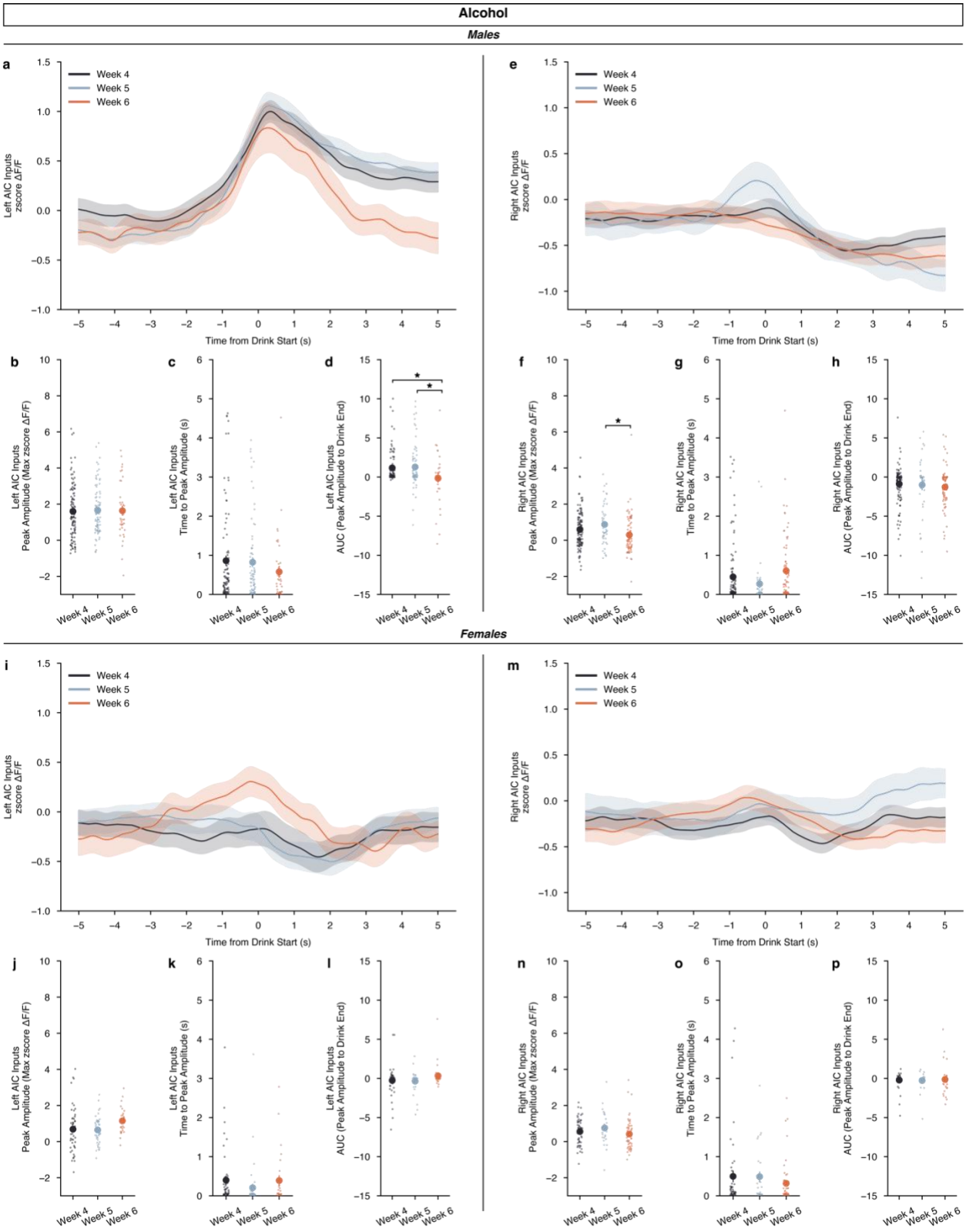

Figure 5: Calcium dynamics of AIC inputs into the left and right DLS across binge alcohol drinking. (a) For males, left AIC inputs to the DLS do not display a week dependent change in ΔF/F

(rmANOVA, DID Week x Time from Drink $F_{(298,298)}$ = 2.271 , p = 0.3729), nor **(b)** did peak amplitudes change by binge week (ANOVA, DID Week $F_{(2,246)}$ = 0.05842, p = 0.9433). No difference in **(c)** time to peak were seen (ANOVA, DID Week $F_{(2,113.7)}$ = 1. 359, p = 0.2609) but **(d)** decreases in AUC were observed in the final binge week compared to the first two (ANOVA, DID Week $F_{(2,91.76)}$ = 3.481, p = 0.03491: Week 4 – Week 6, p = 0.04111; Week 5 – Week 6, p = 0.03777) for male, left AIC inputs. **(e)** Right AIC inputs to the DLS did also not display a by week dependent change in ΔF/F (rmANOVA, DID Week x Time from Drink $F_{(298,596)}$ = 2.166 , p = 0.2743), but **(f)** an increase in peak amplitudes in the second week of binge drinking week was observed in comparison to the final week (ANOVA, DID Week $F_{(2,256)}$ = 4.8388, p = 0.008655; Week 5 – Week 6, p = 0.007429). **(g)** No change in time to peak was observed by week (ANOVA, DID Week $F_{(2,109.8)}$ = 2.933, p = 0.05744) **(h)** and no change in AUC was observed across binge drinking weeks for male, right AIC inputs into the DLS (ANOVA, DID Week $F_{(2,87.91)}$ = 0.5946, p = 0.5539). **(i)** For females, left AIC inputs to the DLS do not display a by week dependent change in ΔF/F (rmANOVA, DID Week x Time from Drink $F_{(298,596)}$ = 1.544, p = 0.3716). **(j)** No change in peak amplitudes, (ANOVA, DID Week $F_{(2,128)}$ = 2.961, p = 0.05534) **(k)** time to peak, (ANOVA, DID Week $F_{(2,70.21)}$ = 1.238, p = 0.2962) or **(l)** AUC were observed (ANOVA, DID Week $F_{(2,69.62)}$ = 2.089, p = 0.1315). **(m)** Right AIC inputs to the DLS did also not display a by week dependent change in ΔF/F (rmANOVA, DID Week x Time from Drink $F_{(298,596)}$ = 0.8997, p = 0.4538). Similar to female, left AIC inputs, there were no changes in **(n)** peak amplitudes, (ANOVA, DID Week $F_{(2,135)}$ = 1.606, p = 0.2045) **(o)** time to peak, (ANOVA, DID Week $F_{(2,70.11)}$ = 1.067, p = 0.3495), or **(p)** AUC by binge drinking week either (ANOVA, DID Week $F_{(2,73.17)}$ = 0. 1216, p = 0.8857). GCaMP activity is aligned to the initiation of the water drinking bout with 5 seconds before and 5 seconds after the bout plotted. Solid lines represent means, and shading or error bars represent the standard error of the mean.

Again, we also split the alcohol data by sex and looked how the development of binge drinking, by week, altered calcium signal. For males, we did not find changes in calcium signal across time from drink start between weeks for either left or right AIC inputs **(Figure 5a & e)**. For left AIC inputs in males, we did not find differences in peak amplitude, time to peak, but we did find a decrease in the off-kinetics in week 6 compared to week 5 and week 4 **(Figure 5b-d)**. This suggests that while alcohol strongly encodes drinking activity during binge alcohol consumption, that the calcium signal begins to decay quicker as drinking history increases. For right AIC inputs, we observed an increase in week 5 compared to week 6 for peak amplitude, but no changes in time to peak or AUC **(Figure 5f-h)**. For females, interestingly, we observed no changes in calcium signal by time for any of the metrics we analyzed **(Figure 5i-p)**. By sex, males show strong engagement of left AIC signals and decreased right AIC signals across increasing binge alcohol history. Further, the left AIC signal's off-kinetics as measured by AUC, decay in the final week of DID, suggesting that long-term exposure to binge alcohol consumption can alter the dynamics of left AIC calcium signals. Yet, for females, across the board, a lack of alcohol-induced changes by time

are observed, which can be interpreted as a resistance or insensitivity to binge alcohol consumption across time.

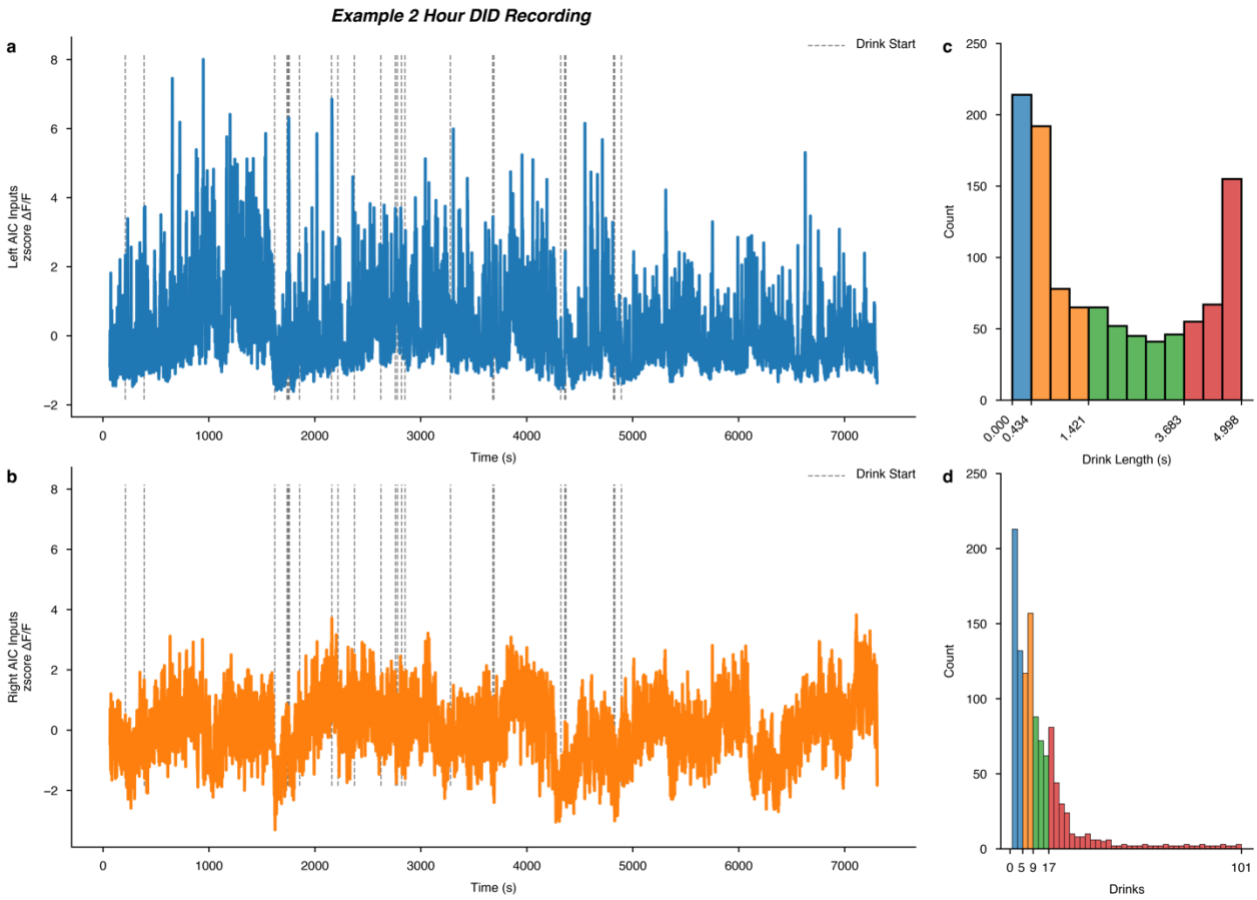

Figure 6: Intra DID session calcium signals and global quantiles of drink length and total number of drinks per session. Example male **(a)** left and **(b)** right AIC input to DLS calcium recordings from a single 2-hour binge alcohol DID recording (animal "P7", session 17), with dashed vertical lines indicating the start of an alcohol drinking event overlayed on the time-resolved GCaMP signal. A histogram of all measured **(c)** drink lengths and **(d)** number of drinks observed across all water and alcohol drinking sessions. On the x-axis, the quartile ranges are printed and colored to visualize the quartile ranges of drink length and total number of drinks that occurred across all water and alcohol DID sessions.

Finally, we wanted to determine if acute water or binge alcohol consumption altered calcium dynamics within a single drinking session. For each DID session, we mapped the start times of drinks onto the full recordings of the left and right AIC input calcium signals. For an example DID session, see **Figure 6a-b**. Then, across all DID sessions, we plotted a histogram of all the drink lengths associated with each drinking event as well as the number of drinks that occurred within all sessions **(Figure 6c-d)**. To compare short versus long drinks and early versus late drinks within DID session, we calculated

the quartile ranges of each measure and assigned those events to their respective range with pseudo colors for easy comparison.

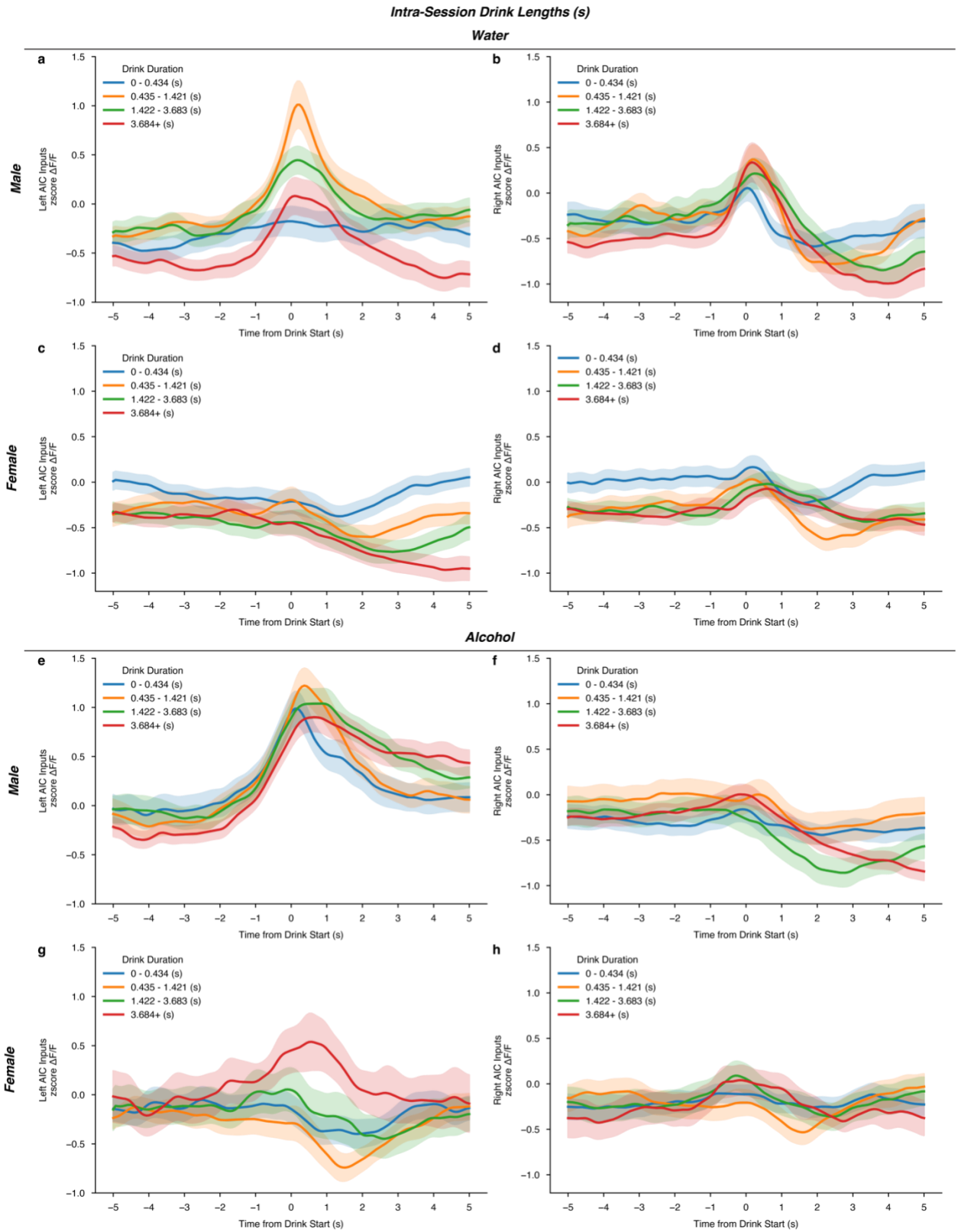

Figure 6 – Figure Supplement 1: Intra DID session calcium signals do not differ by the duration of each drinking event. For water drinking, neither **(a)** left (rmANOVA, Drink Duration x Time from Drink $F_{(596,1192)} = 0.4524$, $p = 0.9999$) or **(b)** right (rmANOVA, Drink Duration x Time from Drink $F_{(596,596)}$

= 0.06445, p = 0.9999) male AIC inputs calcium signals are altered by the length of the drinking event. Nor, do females display any difference in **(c)** left (rmANOVA, Drink Duration x Time from Drink $F_{(596,1788)}$ = 0.1412, p = 0.9999) or **(d)** right (rmANOVA, Drink Duration x Time from Drink $F_{(596,1788)}$ = 0.05649, p = 0.9493) AIC calcium signals by the length of the drinking event. For alcohol drinking events, neither **(e)** left (rmANOVA, Drink Duration x Time from Drink $F_{(447,2682)}$ = 1.594, p = 0.2461) or **(f)** right (rmANOVA, Drink Duration x Time from Drink $F_{(596,596)}$ = 0.8884, p = 0.9557) male AIC inputs calcium signals are altered by the length of the drinking event. Nor, do females display any difference in **(g)** left (rmANOVA, Drink Duration x Time from Drink $F_{(447,1788)}$ = 0.4118, p = 0.9999) or **(h)** right (rmANOVA, Drink Duration x Time from Drink $F_{(447,1788)}$ = 0.5659, p = 0.9999) AIC calcium signals by the length of the alcohol drinking event. GCaMP activity is aligned to the initiation of the water drinking bout with 5 seconds before and 5 seconds after the bout plotted. Solid lines represent means, and shading or error bars represent the standard error of the mean.

We found no differences in calcium signals between sex or fluid as a function of different drink lengths **(Figure 6 – Figure Supplement 1a-h)**. For number of drinks, we also found no differences in calcium signals between sex or fluid as a function of the number of drinks within a single session (**Figure 6 – Figure Supplement 2a-h**). The pattern of calcium activity in male, left AIC inputs into the DLS during binge alcohol drinking is striking, such that it may be the case that increasing acute intoxication decreases the calcium signal seen at these inputs within single DID sessions. However, we did not find statistical evidence of this in our dataset, but this may be because of how we un-biasedly chose to quartile the number of drinks observed and or increasing alcohol tolerance as the number of binge sessions increases for any individual animals' alcohol history. For the purpose and scope of this work, we thought it was important to quantify some basic drinking metrics within DID session to ensure our weekly and between sex and fluid analyses of calcium dynamics were in large part not driven by acute, intra-session effects. Ultimately, we found this to be true, but future work must be done to look at the acute effects of alcohol on AIC inputs within single DID sessions to follow up on these observations.

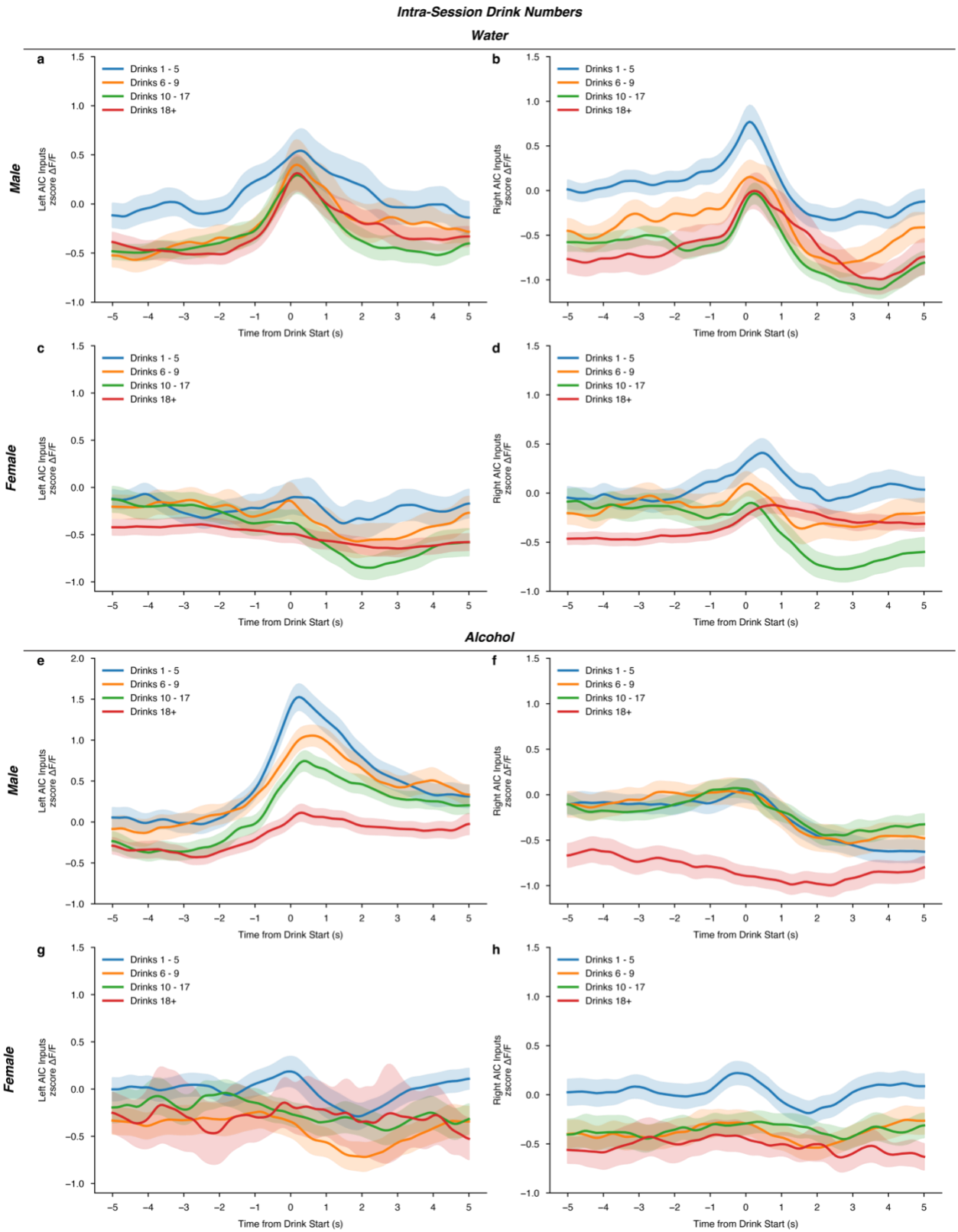

713

714 **Figure–6 - Figure Supplement 2: Intra DID session calcium signals do not differ by the number**
715 **of drinking events within a single session.** For water drinking, neither **(a)** left (rmANOVA, Drink
716 number x Time from Drink $F_{(596,2980)} = 0.8228$, $p = 0.4185$) or **(b)** right (rmANOVA, Drink number x Time

from Drink $F_{(447,1788)} = 1.016$, $p = 0.3921$) male AIC inputs calcium signals are altered by the number of water drinking events within a DID session. Females do not display any difference in **(c)** left (rmANOVA, Drink number x Time from Drink $F_{(447,1341)} = 3.346$, $p = 0.1347$) or **(d)** right (rmANOVA, Drink number x Time from Drink $F_{(447,1341)} = 2.598$, $p = 0.1741$) AIC calcium signals by the increasing number of the drinking events. For alcohol drinking events, neither **(e)** left (rmANOVA, Drink number x Time from Drink $F_{(447,1788)} = 1.608$, $p = 0.2557$) or **(f)** right (rmANOVA, Drink number x Time from Drink $F_{(447,2235)} = 1.664$, $p = 0.2435$) male AIC inputs calcium signals are altered by increasing number of drinking events. Nor, do females display any difference in **(g)** left (rmANOVA, Drink number x Time from Drink $F_{(447,447)} = 0.8444$, $p = 0.5269$) or **(h)** right (rmANOVA, Drink number x Time from Drink $F_{(447,894)} = 0.7267$, $p = 0.5078$) AIC calcium signals by the number of alcohol drinking events. GCaMP activity is aligned to the initiation of the water drinking bout with 5 seconds before and 5 seconds after the bout plotted. Solid lines represent means, and shading or error bars represent the standard error of the mean.

Discussion

In summary, here we show how male and female mice can binge consume both water and alcohol in similar amounts, but via different behavioral strategies. Based on these data, we show how female mice may be more efficient drinkers, more susceptible to inter-session water drinking that modulates future alcohol intake, and time-resolved differences in how their binge drinking behaviors evolve compared to male mice. These robust measurements and resultant sex differences of binge-associated behavioral strategies must continue to be explored, but we hope these data serve as proof for the diversity between sexes that exist in alcohol consumption models even when animals consume similar amounts of alcohol.

The calcium imaging at pre-synaptic AIC inputs to the DLS data presented broadly suggest: 1) there is a time-dependent activation of AIC inputs into the DLS that occurs across drinking weeks where calcium activity, depending on the sex and lateralization, becomes more or less engaged to alcohol drinking and 2) lateralization affects insula projections into the DLS, such that insula signals received in the right and left DLS are remarkably different.

First, we saw strong evidence that AIC inputs into the DLS become engaged around water drinking behaviors, but ultimately most strongly engaged at AIC inputs into the left DLS early in binge alcohol consumption in male mice (**Figure 3c**). Interestingly, these robust calcium signals encoding binge consumption also decayed more rapidly as binge alcohol exposure history increased, suggesting that insular signals into the DLS can dynamically respond to alcohol across time (**Figure 5d**). Together, these data suggest

752 that while AIC inputs into the left DLS are most strongly engaged during alcohol
753 drinking, that the change in their kinetics and thus what they might be encoding in a
754 behavioral and/or interoceptive context may be altered across time due to increasing,
755 repetitive alcohol consumption. And, while these generalized dynamic changes in
756 calcium activity are interesting observations, we did not find strong statistical evidence
757 for changes in calcium signals by week within both water and alcohol drinking across
758 the entire drinking window alone. Thus, while we did find changes in isolated measures
759 such as peak amplitude, time to peak, and AUC by drinking week within water and
760 alcohol drinking, future studies employing faster and higher resolution imaging
761 techniques at cellular resolution, in combination with behavioral paradigms that provide
762 more power at smaller time scales will be needed to understand these changes in
763 calcium dynamics fully. Further, we only measured calcium activity during water and
764 alcohol drinking at AIC inputs into the DLS, but additional work will be required to tease
765 apart changes to glutamate, GABA, and other specific *in-vivo* presynaptic
766 neurotransmitter release in this circuitry as alcohol-induced neuroadaptations form, but
767 nonetheless these data represent intriguing initial findings.

768 Secondly, lateralization of insular activity is well documented in human and rat studies,
769 yet few, if any, mouse studies show clear lateralization effects within the insular cortex
770 (Centanni, Janes et al. 2021). To our knowledge this is the first demonstration, in a
771 water or alcohol drinking paradigm, to show lateralized effects of AIC inputs in the
772 mouse. Also, in our previous work we did not see lateralization effects when stimulating
773 AIC inputs into the left DLS compared to right DLS, but it is important to note that the
774 time-resolution in which we were photoactivating AIC inputs in the DLS was around 10
775 order of magnitudes longer than the time-resolution of the measured calcium activity,
776 suggesting we could have been occluding lateralization effects by stimulating for too
777 long, at a non-biologically relevant frequency, and/or with too much light power
778 (Haggerty, Munoz et al. 2022).

779 Together, these findings suggest there exist both sex-dependent, fluid-dependent, and
780 brain lateralization effects for AIC inputs into the DLS in how they encode water and
781 alcohol drinking activity. Here, we mainly focused on describing increases in calcium
782 activity and its associated dynamics to demonstrate how male, left AIC inputs into the

783 DLS are more robustly engaged during binge drinking behaviors. But, we also reported
784 many instances where calcium signals were decreased, where shifts in time to peaks
785 occurred, and where sustained decreases in calcium signals occurred for many
786 seconds post drinking initiation, especially on right AIC inputs in both males and
787 females. It is known that these shifts, pauses, and decreases in firing can also have
788 profound behavioral effects, and likely are interacting with the increases in calcium
789 activity described to direct a concert of action selection behaviors relevant for both
790 alcohol and water drinking behaviors. Again, work utilizing higher resolution *in-vivo*
791 imaging and behavioral assays and analyses will be required to resolve these changes,
792 but nonetheless these observations provide initial evidence for a powerful, complex
793 cortico-striatal circuit that has vast implications in addiction-related behaviors.

794 Further, the findings presented here help contextualize our previous work on AIC input
795 control over binge alcohol drinking behaviors such that alcohol exposure in males
796 decreases robust calcium activity from AIC inputs that when restored with
797 photoactivation of AIC inputs into the DLS leads to decreases in binge alcohol
798 consumption **(Figure 5d)**. Yet, in females the lack of perturbed calcium dynamics may
799 correlate with the lack of alcohol-induced changes in synaptic plasticity that were
800 observed in slice electrophysiology at AIC inputs to the DLS after 3 weeks of binge
801 alcohol exposure (Haggerty, Munoz et al. 2022). In conclusion, leveraging these sex-
802 dependent differences in AIC circuitry as binge drinking behaviors develop may
803 represent novel biological levers to target in the quest for developing new
804 pharmacotherapies and therapeutic modalities to treat those experiencing AUD.

Author Contributions

DLH: Conceptualization, Resources, Data Curation, Software, Formal Analysis, Funding Acquisition, Investigation, Visualization, Methodology, Writing - Original Draft, Project Administration, Writing – Review and Editing

BKA: Conceptualization, Supervision, Funding Acquisition, Methodology, Project Administration, Writing – Review and Editing

Funding

National Institutes of Health (R01AA027214) - BKA; National Institutes of Health (F31AA029297) – DLH; National Institutes of Health (T32AA07462) - DLH

Competing Interests

No competing interests declared

References

Abadi, M., P. Barham, J. Chen, Z. Chen, A. Davis, J. Dean, M. Devin, S. Ghemawat, G. Irving, M. Isard, M. Kudlur, J. Levenberg, R. Monga, S. Moore, D. G. Murray, B. Steiner, P. Tucker, V. Vasudevan, P. Warden, M. Wicke, Y. Yu and X. Zheng (2016). TensorFlow: a system for large-scale machine learning. Proceedings of the 12th USENIX conference on Operating Systems Design and Implementation. Savannah, GA, USA, USENIX Association**:** 265–283.

Addolorato, G., G. A. Vassallo, G. Antonelli, M. Antonelli, C. Tarli, A. Mirijello, A. Agyei-Nkansah, M. C. Mentella, D. Ferrarese, V. Mora, M. Barbara, M. Maida, C. Camma, A. Gasbarrini and C. Alcohol Related Disease (2018). "Binge Drinking among adolescents is related to the development of Alcohol Use Disorders: results from a Cross-Sectional Study." Sci Rep **8**(1): 12624.

Ardinger, C. E., C. C. Lapish, C. L. Czachowski and N. J. Grahame (2022). "A critical review of front-loading: A maladaptive drinking pattern driven by alcohol's rewarding effects." Alcohol: Clinical and Experimental Research **46**(10): 1772-1782.

Barkley-Levenson, A. M. and J. C. Crabbe (2014). "High drinking in the dark mice: a genetic model of drinking to intoxication." Alcohol **48**(3): 217-223.

Blednov, Y. A., P. Metten, D. A. Finn, J. S. Rhodes, S. E. Bergeson, R. A. Harris and J. C. Crabbe (2005). "Hybrid C57BL/6J x FVB/NJ mice drink more alcohol than do C57BL/6J mice." Alcoholism, clinical and experimental research **29**(11): 1949-1958.

Burnham, N. W., C. N. Chaimowitz, C. C. Vis, A. P. Segantine Dornellas, M. Navarro and T. E. Thiele (2021). "Lateral hypothalamus-projecting noradrenergic locus coeruleus pathway modulates binge-like ethanol drinking in male and female TH-ires-cre mice." Neuropharmacology **196**: 108702.

Centanni, S. W., A. C. Janes, D. L. Haggerty, B. Atwood and F. W. Hopf (2021). "Better living through understanding the insula: Why subregions can make all the difference." Neuropharmacology **198**: 108765.

Czerniak, R. (2001). "Gender-based differences in pharmacokinetics in laboratory animal models." Int J Toxicol **20**(3): 161-163.

Dornellas, A. P. S., N. W. Burnham, K. L. Luhn, M. V. Petruzzi, T. E. Thiele and M. Navarro (2021). "Activation of locus coeruleus to rostromedial tegmental nucleus (RMTg) noradrenergic pathway blunts binge-like ethanol drinking and induces aversive responses in mice." Neuropharmacology **199**: 108797.

Elvig, S. K., M. A. McGinn, C. Smith, M. A. Arends, G. F. Koob and L. F. Vendruscolo (2021). "Tolerance to alcohol: A critical yet understudied factor in alcohol addiction." Pharmacol Biochem Behav **204**: 173155.

Ferguson, L. B., L. Zhang, D. Kircher, S. Wang, R. D. Mayfield, J. C. Crabbe, R. A. Morrisett, R. A. Harris and I. Ponomarev (2019). "Dissecting Brain Networks Underlying Alcohol Binge Drinking Using a Systems Genomics Approach." Mol Neurobiol **56**(4): 2791-2810.

Finn, D. A., M. L. Helms, M. A. Nipper, A. Cohen, J. P. Jensen and L. L. Devaud (2018). "Sex differences in the synergistic effect of prior binge drinking and traumatic stress on subsequent ethanol intake and neurochemical responses in adult C57BL/6J mice." Alcohol **71**: 33-45.

858 Godynyuk, E., M. N. Bluitt, J. R. Tooley, A. V. Kravitz and M. C. Creed (2019). "An Open-Source,
859 Automated Home-Cage Sipper Device for Monitoring Liquid Ingestive Behavior in Rodents."
860 eNeuro **6**(5): ENEURO.0292-0219.2019.
861 Grecco, G. G., D. L. Haggerty, K. C. Reeves, Y. Gao, D. Maulucci and B. K. Atwood (2022).
862 "Prenatal opioid exposure reprograms the behavioural response to future alcohol reward."
863 Addiction Biology **27**(2): e13136.
864 Haggerty, D. L., B. Munoz, T. Pennington, G. Viana Di Prisco, G. G. Grecco and B. K. Atwood
865 (2022). "The role of anterior insular cortex inputs to dorsolateral striatum in binge alcohol
866 drinking." Elife **11**: e77411.
867 Hunter, J. D. (2007). "Matplotlib: A 2D Graphics Environment." Computing in Science &
868 Engineering **9**(3): 90-95.
869 Huynh, N., N. M. Arabian, L. Asatryan and D. L. Davies (2019). "Murine drinking models in the
870 development of pharmacotherapies for alcoholism: drinking in the dark and two-bottle choice."
871 JoVE (Journal of Visualized Experiments)(143): e57027.
872 Hwa, L. S., A. Chu, S. A. Levinson, T. M. Kayyali, J. F. DeBold and K. A. Miczek (2011). "Persistent
873 escalation of alcohol drinking in C57BL/6J mice with intermittent access to 20% ethanol."
874 Alcohol Clin Exp Res **35**(11): 1938-1947.
875 Kanny, D., T. S. Naimi, Y. Liu, H. Lu and R. D. Brewer (2018). "Annual Total Binge Drinks
876 Consumed by U.S. Adults, 2015." Am J Prev Med **54**(4): 486-496.
877 Keyes, K. M., J. Jager, T. Mal-Sarkar, M. E. Patrick, C. Rutherford and D. Hasin (2019). "Is There a
878 Recent Epidemic of Women's Drinking? A Critical Review of National Studies." Alcohol Clin Exp
879 Res **43**(7): 1344-1359.
880 Levine, O. B., M. J. Skelly, J. D. Miller, J. K. Rivera-Irizarry, S. A. Rowson, J. F. DiBerto, J. A. Rinker,
881 T. E. Thiele, T. L. Kash and K. E. Pleil (2021). "The paraventricular thalamus provides a
882 polysynaptic brake on limbic CRF neurons to sex-dependently blunt binge alcohol drinking and
883 avoidance behavior in mice." Nat Commun **12**(1): 5080.
884 Mokdad, A. H., J. S. Marks, D. F. Stroup and J. L. Gerberding (2004). "Actual causes of death in
885 the United States, 2000." JAMA **291**(10): 1238-1245.
886 Munoz, B., B. M. Fritz, F. Yin and B. K. Atwood (2018). "Alcohol exposure disrupts mu opioid
887 receptor-mediated long-term depression at insular cortex inputs to dorsolateral striatum." Nat
888 Commun **9**(1): 1318.
889 Overstreet, D. H., D. J. Knapp and G. R. Breese (2004). "Modulation of multiple ethanol
890 withdrawal-induced anxiety-like behavior by CRF and CRF1 receptors." Pharmacol Biochem
891 Behav **77**(2): 405-413.
892 Pedregosa, F., G. Varoquaux, A. Gramfort, V. Michel, B. Thirion, O. Grisel, M. Blondel, P.
893 Prettenhofer, R. Weiss and V. Dubourg (2011). "Scikit-learn: Machine learning in Python." the
894 Journal of machine Learning research **12**: 2825-2830.
895 Rinker, J. A., S. A. Marshall, C. M. Mazzone, E. G. Lowery-Gionta, V. Gulati, K. E. Pleil, T. L. Kash,
896 M. Navarro and T. E. Thiele (2017). "Extended Amygdala to Ventral Tegmental Area
897 Corticotropin-Releasing Factor Circuit Controls Binge Ethanol Intake." Biol Psychiatry **81**(11):
898 930-940.
899 Satta, R., E. R. Hilderbrand and A. W. Lasek (2018). "Ovarian hormones contribute to high levels
900 of binge-like drinking by female mice." Alcoholism: Clinical and Experimental Research **42**(2):
901 286-294.

Savarese, A. M., A. R. Ozburn, A. M. Barkley-Levenson, P. Metten and J. C. Crabbe (2021). "The impact of Drinking in the Dark (DID) procedural manipulations on ethanol intake in High Drinking in the Dark (HDID) mice." Alcohol **93**: 45-56.

Schramm-Sapyta, N. L., Q. D. Walker, J. M. Caster, E. D. Levin and C. M. Kuhn (2009). "Are adolescents more vulnerable to drug addiction than adults? Evidence from animal models." Psychopharmacology (Berl) **206**(1): 1-21.

Seabold, S. and J. Perktold (2010). Statsmodels: Econometric and statistical modeling with python. Proceedings of the 9th Python in Science Conference, Austin, TX.

Siciliano, C. A., H. Noamany, C. J. Chang, A. R. Brown, X. Chen, D. Leible, J. J. Lee, J. Wang, A. N. Vernon, C. M. Vander Weele, E. Y. Kimchi, M. Heiman and K. M. Tye (2019). "A cortical-brainstem circuit predicts and governs compulsive alcohol drinking." Science **366**(6468): 1008-1012.

Sneddon, E. A., R. D. White and A. K. Radke (2019). "Sex Differences in Binge-Like and Aversion-Resistant Alcohol Drinking in C57BL/6J Mice." Alcohol Clin Exp Res **43**(2): 243-249.

Thiele, T. E. and M. Navarro (2014). ""Drinking in the dark" (DID) procedures: a model of binge-like ethanol drinking in non-dependent mice." Alcohol **48**(3): 235-241.

Vallat, R. (2018). "Pingouin: statistics in Python." Journal of Open Source Software **3**(31): 1026.

Vandegrift, B. J., E. R. Hilderbrand, R. Satta, R. Tai, D. He, C. You, H. Chen, P. Xu, C. Coles, M. S. Brodie and A. W. Lasek (2020). "Estrogen Receptor α Regulates Ethanol Excitation of Ventral Tegmental Area Neurons and Binge Drinking in Female Mice." The Journal of Neuroscience **40**(27): 5196-5207.

Virtanen, P., R. Gommers, T. E. Oliphant, M. Haberland, T. Reddy, D. Cournapeau, E. Burovski, P. Peterson, W. Weckesser, J. Bright, S. J. van der Walt, M. Brett, J. Wilson, K. J. Millman, N. Mayorov, A. R. J. Nelson, E. Jones, R. Kern, E. Larson, C. J. Carey, I. Polat, Y. Feng, E. W. Moore, J. VanderPlas, D. Laxalde, J. Perktold, R. Cimrman, I. Henriksen, E. A. Quintero, C. R. Harris, A. M. Archibald, A. H. Ribeiro, F. Pedregosa, P. van Mulbregt and C. SciPy (2020). "SciPy 1.0: fundamental algorithms for scientific computing in Python." Nat Methods **17**(3): 261-272.

Waskom, M. L. (2021). "Seaborn: statistical data visualization." Journal of Open Source Software **6**(60): 3021.

White, A. M. (2020). "Gender Differences in the Epidemiology of Alcohol Use and Related Harms in the United States." Alcohol Res **40**(2): 01.